Anticipating Climate Change Across the United States[*]

Adrien Bilal   Esteban Rossi-Hansberg

Harvard University   *University of Chicago*

June 1, 2023

Abstract

We evaluate how anticipation and adaptation shape the aggregate and local costs of climate change. We develop a dynamic spatial model of the U.S. economy and its 3,143 counties that features costly forward-looking migration and capital investment decisions. Recent methodological advances that leverage the 'Master Equation' representation of the economy make the model tractable. We estimate the county-level impact of severe storms and heat waves over the 20th century on local income, population, and investment. The estimated impact of storms matches that of capital depreciation shocks in the model, while heat waves resemble combined amenity and productivity shocks. We then estimate migration and investment elasticities, as well as the structural damage functions, by matching these reduced-form results in our framework. Our findings show, first, that the impact of climate on capital depreciation magnifies the U.S. aggregate welfare costs of climate change twofold to nearly 5% in 2023 under a business-as-usual warming scenario. Second, anticipation of future climate damages amplifies climate-induced worker and investment mobility, as workers and capitalists foresee the slow build-up of climate change. Third, migration reduces substantially the spatial variance in the welfare impact of climate change. Although both anticipation and migration are important for local impacts, their effect on aggregate U.S. losses from climate change is small.

1 Introduction

The accumulation of CO_2 in the atmosphere is affecting the climate of our planet. Some of these effects are evident today, but many others, including the increased frequency and intensity of storms and heat waves (IPCC, 2022), are expected over the next century as the Earth's average temperature increases further. The fact that humans today can anticipate these future climate effects can have profound implications on their ability to adapt and reduce their worse consequences. What is the importance of these anticipatory and adaptive responses in determining the aggregate and local costs of climate change? In this paper, we answer this question using a general equilibrium dynamic quantitative spatial model of the 3,143 counties in the U.S. economy. In our framework, agents anticipate the effect of climate change on productivity and capital depreciation and make forward-looking migration and local capital investment decisions. We also provide novel empirical estimates of the local impact of storms and heat waves on economic activity, which we use to quantify the model.

The analysis of anticipatory and adaptation responses to climate change at this level of spatial resolution has previously been hindered by the dimensionality of the resulting state space. In a dynamic model with costly forward-looking migration and local capital investment decisions, the whole distribution of employment and capital are state variables in the dynamic problem of individual workers and local capital investors. Connecting such a framework with micro-level estimates of the impact of storms and heat waves requires a fine level of spatial disaggregation. To make progress, we leverage recent methodological advances developed in Bilal (2021) that allow us to solve for quantitative general equilibrium counterfactuals in heterogeneous agent models with aggregate shocks using analytic first-order perturbations around the initial deterministic steady-state. With this technique in hand, we develop a framework to evaluate the impact of climate change on the U.S. economy.

Our starting point is a standard forward-looking dynamic migration model as in Caliendo et al. (2019). Forward-looking workers decide where to live and work. They earn an equilibrium wage in their location that they use to consume and lease housing at equilibrium rents. They receive random preference shocks for locations that motivate them to migrate subject to bilateral migration costs. We enrich this environment along several dimensions. First, as in Kleinman et al. (2023), we introduce local capitalists who own the capital stock in the location where they live. They face a dynamic consumption-investment decision subject to adjustment costs that accounts for the entire future expected path of the economy and the evolution of its climate. The evolution of the local paths of capital depreciation rates, productivities and amenities depends on climate change through its effect on storms and heat waves. Capitalists rent out their capital stock to developers who use it to produce housing and commercial structures. Local firms produce consumption goods using labor and commercial structures with productivity that is heterogeneous across locations and varies with global temperatures.

An essential part of the quantification of this model is our estimation of damage functions that map

global temperature changes into local changes in capital depreciation rates, productivity, and amenities. We collect daily data on mean and extreme temperature, precipitation, and windspeed for every county in the U.S. since 1900. We use these data to construct county-level indicators of 1-in-50-years storms, and 1-in-20-years heat waves. We document that the probability of storms in coastal counties, and heat waves in warm (above-median) counties in the U.S. has risen fourfold with the 1°C of global warming the planet experienced in the last century.

We then estimate the impact of these extreme events on economic activity from the year 2000 onwards using an event study design. Specifically, we use a distributed lag specification to estimate how income per capita, population, and investment respond to extreme events conditional on a rich set of controls. We find that storms reduce income per capita by over 2% and population by 5%, while investment rises to peak at a 20% increase. These effects are concentrated in coastal counties, precisely where storms are becoming more frequent. Together, these patterns are consistent with a capital depreciation shock in the model. Heat waves reduce income per capita and population by 2%, and investment by 4%, in counties with temperatures above the median where their frequency is rising. These results are consistent with a combination of negative productivity and amenity shocks in the model.

We use these reduced-form estimates to quantify our framework. We first estimate the migration and investment elasticities. Given a guess for these elasticities, and a standard calibration of the rest of the model parameters, we can invert the model in steady-state, and obtain all the local characteristics, including local productivities, amenities, and the level of local capital investment costs. To estimate the two elasticities, we leverage a key property of the first-order approximation of changes in our economy around the steady state, namely, that the *relative* response of economic outcomes to shocks is independent of the magnitude of the shock. Hence, we estimate these elasticities by matching the estimated reduced-form response of population, relative to income per capita and investment, to storms and heat waves. We leverage the computational efficiency of our solution method to propose global identification guarantees.

We then proceed to estimate the damage functions. We recover the magnitude of the capital depreciation, productivity, and amenity shocks corresponding to a 1-in-50-years storm and a 1-in-20 years heat wave by matching the *level* of the cumulative impulse response of investment and population in the model to the one we estimated in the data over a 10-year period. The final step is to interact damages from a given event with changes in the empirical probability that a given event materializes for each location in response to changes in temperature.

Storms and heat waves have large effects on capital depreciation, productivity, and amenities. Through the lens of our model, storms generate a 17% capital depreciation shock, while heat waves generate a 5.1% productivity shock together with a 6.8% amenity shock. The resulting structural damage functions imply that the South-Eastern Atlantic coast should expect a 2 to 4 p.p. increase in the annual capital depreciation rate for every 1°C increase in global mean temperatures because of rising storm activity. Southern Florida should expect a 5% reduction in productivity, and a 6.6% reduction in amenities, for

every 1°C increase in global mean temperature.

We use the quantified model to evaluate the social cost of climate change in the U.S. economy. Our central scenario is a gradual increase of global mean temperature from 1°C to 4°C above pre-industrial levels by 2100, consistent with the IPCC's business-as-usual scenario. In our baseline counterfactual, the consumption-equivalent present discounted welfare of workers falls by 4.9% on average in 2023 ($3,005 per year per worker). Despite the ability of workers to migrate away from affected areas, there is substantial dispersion across counties. The standard deviation of welfare losses for workers is 2.4 p.p. Capitalists lose 0.8% on average but face much larger inequality: a standard deviation of losses of 5.6 p.p in 2023 and of 46.4 p.p. by 2100. Losses to capitalists are more dispersed because physical capital cannot be moved directly: it is left to depreciate in impacted areas such as southern Florida and rebuilt in less affected areas such as inland Maine. By 2100, average welfare losses reach 11.6% for workers ($7,115 per year per worker) and 13.4% for capitalists. These large welfare losses occur despite sizable population and capital flows. By 2100, the population has changed by 40% on average across all counties due to climate change; the aggregate capital stock of the U.S. economy has declined by 32%.

Our goal is to gauge the importance of anticipation and adaptation responses in determining these results. To do so, we perform three distinct exercises in which we shut down particular channels in the model. First, we shut down the effect of storms on capital depreciation. This allows us to assess the relevance of incorporating capital in a climate assessment model. The effect of changes in global temperature on capital depreciation alone accounts for 88% of welfare losses to capitalists, 45% of welfare losses to workers, and 75% of the aggregate reduction in capital by 2100. The destruction created by storms through changes in local capital depreciation rates is a novel feature of our analysis, and this channel turns out to be quantitatively critical to account accurately for expected losses from climate change.

In a second exercise, we shut down climate change anticipation by workers and capitalists. In this counterfactual, agents experience the effect of the current and past changes in temperatures but they believe that in the future temperatures will remain as in the current period. Hence, their actions incorporate no anticipation effects. Our results indicate that anticipation plays a crucial role for mobility and investment. Without anticipation, mobility drops by 32%. There are two main reasons. First, workers fail to out-migrate enough from locations that will become less attractive as the climate worsens. Second, capitalists keep investing in these same locations, raising the incentives for workers to stay there. Without anticipation, welfare is 13% more dispersed across locations. For example, workers in Florida lose an additional 0.65% of consumption equivalent welfare. Nevertheless, gains in some locations offset losses in others, yielding similar aggregate welfare losses.

In the third and final exercise, we measure the importance of adaptation through migration for the spatial distribution of county losses from climate change. To do so, we simply prevent people from moving in response to climate change, while capital can adjust as in the baseline. Without migration,

the distribution of welfare losses for workers spreads out substantially. Across the U.S., the standard deviation of worker welfare losses in 2023 rises to 8.7 p.p and to 16.3 p.p in 2100. Workers in particularly adversely affected areas, such as coastal counties in Florida and Louisiana, experience losses of 25% in 2023 instead of 5%, corresponding to an additional loss of \$12,267 per year per capita. In contrast, since capital stocks are not mobile, the lack of mobility of workers insures local capitalists in affected areas. Hence, the dispersion in capitalist welfare declines more than threefold in 2023 and by half in 2100. Our results point to a dynamic complementarity between migration and investment decisions that shapes the spatial distribution of winners and losers of climate change.

Perhaps surprisingly, shutting down migration has only a negligible effect on the average welfare loss of either workers or capitalists. The gains in some locations compensate for the losses in others. We propose an exact welfare decomposition that yields two observations. First, at the individual level, the option value of migration nets out on average due to an envelope argument: the marginal mover is already indifferent between their preferred and runner-up location prior to climate change. Second, at the aggregate level, migration provides insurance only if climate shocks reallocate workers toward more desirable locations. We find that, in the U.S., the correlation between the impact of climate change and current economic development and welfare is close to zero, implying negligible aggregate benefits from migration.[1]

The methodology that allows us to reach these conclusions is related to the literature on mean-field games. Together, the elements of our framework represent a heterogeneous agent environment with aggregate shocks in which the full distribution of workers and capital stocks across counties matters for the evolution of the economy. Standard solution methods are not well-suited the dimensionality of this framework. To make progress, we leverage recent methodological advances developed in Bilal (2021) that leverage the 'Master Equation' representation of the economy, itself introduced in the mathematics mean field games literature (Cardaliaguet et al., 2019).[2] We take analytic first-order perturbations of the Master Equation in aggregate temperature shocks and in the underlying distribution around the initial deterministic steady-state to obtain low-dimensional, closed-form standard Bellman equations for the directional derivatives of individual value functions with respect to the underlying distribution and aggregate shocks.[3]

Our paper is also related to the literature on dynamic spatial models. Relative to Desmet et al. (2018), our methodology allows us to introduce forward-looking decisions in migration and capital investments, although we abstract from agglomeration effects in productivity, and technology innovations, and focus our

---

[1]Desmet and Rossi-Hansberg (2015), Desmet et al. (2021), and Cruz and Rossi-Hansberg (2023) reach different conclusions on the importance of migration to determine the aggregate losses from climate change in the world since the correlation between income per capita and the magnitude of negative climate shocks in the world is substantial and positive. The absence of static and dynamic agglomeration effects in productivity or amenities is also important for positive and negative local effects to average out.

[2]The 'Master Equation' representation is the recursive representation of the economy, in which the distribution of workers and capital stocks enters explicitly as an explicit state variable of the individual decision problems.

[3]The Master Equation approach in Bilal (2021) is also related to the Reiter (2009) method. By taking the perturbation analytically rather than numerically, the Master Equation approach is simpler and faster, which is particularly useful for estimating the parameters of the model.

analysis on the U.S. Caliendo et al. (2019) introduces forward-looking migration decisions and Kleinman et al. (2023) adds local capital investments. Both of them also introduce costly trade, which we abstract from. Relative to these papers our methodology allows us to efficiently compute counterfactuals for a much larger number of locations (all counties in the U.S. v.s. 50 states). Perhaps more important, the efficient numerical solution allows us to estimate the two key elasticities, and the climate damage functions, by precisely matching the model results with the reduced-form local responses that we estimate in the data.

Of course, the main contribution of our paper is to evaluate the economic losses due to the capital depreciation generated by storms, together with the productivity and amenity losses due to heat waves. We aim to analyze the role of anticipation and adaptation in determining aggregate and local losses as well as the resulting migration flows and geography of investments. In doing so, we also contribute to the reduced-form literature that estimates the impact of storms (Deryugina, 2013, Hsiang and Jina, 2014, Roth Tran and Wilson, 2023, Phan and Schwartzman, 2023) and extreme heat (Deschênes and Greenstone, 2011, Dell et al., 2012, Dell et al., 2014) by providing comprehensive county-level estimates for the U.S. of the effect of storms on coastal counties and heat waves in warm counties.

We incorporate our reduced-form estimates into a general equilibrium dynamic spatial climate assessment model to estimate structural damage functions. A recent literature has proposed related frameworks. Many of those papers focus on other issues and abstract completely from capital investments or anticipations effects (Desmet and Rossi-Hansberg, 2015, Desmet et al., 2021, Cruz and Rossi-Hansberg, 2023, and Conte et al., 2022). Cruz (2021) and Balboni (2021) study the effect of temperature changes and flooding, respectively, in models with forward-looking migration but abstract from local capital accumulation. Rudik et al. (2022) also incorporates forward-looking migration and trade and calculates the impact of climate change in the U.S. on productivity and welfare using trade and migration flows, but also abstract from capital investments and capital depreciation shocks. In contrast, Krusell and Smith (2022) propose a model of the effect of climate change on local capital investments for the entire world but abstract from migration or the capital destruction shocks generated by floods and storms.[4] Fried (2021) evaluates the impact of storms in an incomplete credit market model with adaptation across two regions. Relative to this literature, we are the first to propose a spatially disaggregated dynamic model with both migration and capital investments to quantify the effect of climate-change-induced storms and heat waves in the U.S., and use it to gauge the role of anticipation and adaptation in determining the size and spatial distribution of these losses.

The rest of this paper is organized as follows. Section 2 lays out the model. Section 3 characterizes our solution method. Section 4 describes our reduced-form results. Section 5 details our quantification procedure. Section 6 presents our three main results. Section 7 concludes.

---

[4]See also Bakkensen and Barrage (2018) for a study of the impact of storms in a multi-country setting.

2 A model of location and investment choices in a warming world

This section presents the setup of our dynamic spatial model. We model an economy with many locations and two types of agents: workers and capitalists. Workers can move subject to mobility costs and earn a wage that they consume each period. Capitalists are fixed in a location, earn the returns on their capital investments, and face a dynamic consumption-savings decision. We now proceed to describe each part of our setup in detail.

2.1 Agents and preferences

There is a unit mass of infinitely-lived workers who choose in which location $i \in \{1, ..., \mathcal{I}\}$ to live. Workers living in location i have CRRA preferences $A_{it} + u(C) = A_{it} + \frac{C^{1-\gamma}-1}{1-\gamma}$ over amenities A_{it} in the location where they live at time t and a Cobb-Douglas aggregator C of a freely traded final good, used as the numeraire, and housing. Namely, $C = \left(\frac{c}{1-\beta}\right)^{1-\beta} \left(\frac{h}{\beta}\right)^{\beta}$, where β denotes the share of housing in expenditure. Workers discount the future at rate ρ. Workers are allowed to move at rate μ, in which case they draw extreme-value distributed idiosyncratic preference shocks for potential destinations, with dispersion parameter ν. If they move, they pay a bilateral moving cost τ_{ij}. We define the long-run (A_i) and time-varying (a_{it}) components of amenities in location i as $A_{it} = A_i + a_{it}$.

Each location is populated by a unit measure of capitalists. They are immobile and have risk-neutral preferences $u^{\text{cap}}(C) = C$ over the final consumption good. They do not consume housing.

2.2 Technology

Workers in location i are employed by a representative firm that produces the final good using commercial structures and labor and faces constant returns to scale. Locations are endowed with a local productivity Z_{it} and a local stock of land L_i. A representative firm is endowed with a production function for the final good given by $Y_{it} = Z_{it}S_{it}^{\alpha}(N_{it}^P)^{1-\alpha}$, where S_{it} denotes local commercial structures and N_{it}^P the local number of workers employed in final good production. We denote by N_{it} the total number of workers in location i at time t. We define the long-run (Z_i) and time-varying (χ_{it}) components of productivity as $Z_{it} \equiv Z_i e^{\chi_{it}}$.

In every location, there is an equilibrium capital stock K_{it}. Capital can be combined with land L_i and construction labor N_{it}^B to produce buildings B_{it} according to the production function $B_{it} = L_i^{\omega}(N_{it}^B)^{\varpi}K_{it}^{1-\omega-\varpi}$. Buildings B_{it} can be costlessly repurposed between residential housing and commercial structures, so that $B_{it} = S_{it} + H_{it}$. Denote by r_{it} the common rental rate of buildings to firms and workers.

Capitalists decide how much to invest in every location subject to constant returns to scale investment costs, convex in I, $c_i(I/K)K = \frac{c_{i0}^{-1/\zeta}}{1+1/\zeta}\left(\frac{I}{K}\right)^{1+1/\zeta}K$. These costs are paid in the final good whose price is normalized to 1. To finance investment, capitalists borrow or save in a risk-free national bond market which carries an equilibrium interest rate $\overline{R}_t$. Capital is not mobile across locations. We denote by $R_{K,it}$

the return on a unit of capital. The local capital stock depreciates at rate Δ_{it}. We define the long-run (Δ_i) and time-varying (δ_{it}) components of capital depreciation rates as $\Delta_{it} \equiv \Delta_i + \delta_{it}$.

Capitalists are endowed with non-traded shares of a national mutual fund. This mutual fund owns the land in the economy. Denote by θ_{it} the payment from the mutual fund to capitalists in location i at time t.

2.3 Climate change

The path of global mean temperatures T_t is exogenous. Going forward, the vast majority of carbon emissions is expected to stem from developing economies and is thus largely exogenous to U.S. economic activity. Global mean temperatures relative to pre-industrial levels T^P satisfy

$$T_t - T^P = \epsilon(z_t + T_t^D).$$

T_t^D is a deterministic path corresponding to a central climate scenario. z_t is a mean-zero shock that captures natural climate variability. ϵ is a scaling parameter that clarifies notation for our solution method.[5]

Local productivity χ_{it}, amenities a_{it}, and capital depreciation δ_{it} depend on time only through the path of global mean temperatures. We parameterize these shifters through the following functions:

$$\chi_{it} = \chi_i\left(T_t - T^P\right), \qquad a_{it} = a_i\left(T_t - T^P\right), \qquad \delta_{it} = \delta_i\left(T_t - T^P\right), \tag{1}$$

where $\chi_i(0) = a_i(0) = \delta_i(0) = 0$. Even though these damages functions take global temperature as an argument, they capture flexibly the possible dependence of damages on local temperature through their location index i.[6]

2.4 Static equilibrium

The maximization probrem of firms implies that the wage w_{it} in location i satisfies the firm's first-order condition $w_{it} = (1-\alpha)Z_{it}(S_{it}/N_{it}^P)^\alpha$. Similarly, the rental rate for structures satisfies $r_{it} = \alpha Z_{it}(S_{it}/N_{it}^P)^{-(1-\alpha)}$, since depreciation is not covered by the users of buildings.

The optimal choice of labor in building production implies $\varpi r_{it} B_{it}/N_{it}^B = w_{it}$. Furthermore, the local demand for housing by workers implies that an equilibrium in the housing market satisfies $\beta w_{it} N_{it} = r_{it} H_{it}$.

---

[5]We could introduce uncertainty in the long-run path of temperatures by writing $T_t - T^P = \epsilon(z_t + \tilde{z}_t T_t^D)$ for some process $\tilde{z}_t$. Since our solution method relies on a first-order perturbation of the economy, such uncertainty would be immaterial for our results. Uncertainty matters for higher-order perturbations.

[6]For instance, they are equivalent to positing that damages are a function of local temperature deviations (e.g. $\chi_{it} = F(T_{it} - \overline{T}_i)$) and that local temperature is related to global temperature according to $T_{it} = \overline{T}_i + \overline{\tau}_i(T_t - T^P)$.

We determine equilibrium prices and quantities as functions of the local capital stock K_{it} and local number of workers N_{it}. We show that labor is allocated to goods and buildings production in constant shares: $N_{it}^P = x N_{it}$ and $H_{it} = y B_{it}$, where x, y are combinations of parameters described in equation (21), Appendix A.1.

Using these shares and the production function of buildings, the wage and the rental rate of buildings become

$$w_{it} = w_{i0} Z_{it} L_i^{\omega\alpha}(K_{it}^{1-\omega-\varpi}N_{it}^{\varpi-1})^\alpha \quad , \quad r_{it} = r_{i0} Z_{it} L_i^{-\omega(1-\alpha)}(K_{it}^{1-\omega-\varpi}N_{it}^{\varpi-1})^{-(1-\alpha)}, \tag{2}$$

where w_{i0}, r_{i0} are combinations of parameters and local fundamentals expressed in Appendix A.1.

We solve for the rental rate of capital. It depends on the rental rate of buildings. Profit maximization by developers implies that it satisfies:

$$R_{K,it} = R_{0i} e^{\chi_{it}} K_{it}^{-\phi} N_{it}^\psi \equiv R_i(\chi_{it}, K_{it}, N_{it}),$$

where R_{0i} is a location-specific constant that depends on the permanent component of productivity and available land, and ϕ and ψ are combinations of parameters detailed in Appendix A.1.

We can now solve for consumption given prices. Consumption in location i is equal to the real wage. It satisfies

$$C_{it} = \frac{w_{it}}{r_{it}^\beta} = C_{0i} e^{(1-\beta)\chi_{it}} \left(\frac{K_{it}^{1-\omega-\varpi}}{N_{it}^{1-\varpi}}\right)^\xi,$$

where C_{0i} is a location-specific constant, and ξ a combination of parameters detailed in Appendix A.1. Finally, flow utility in location i at time t is:

$$A_{it} + u\left(\frac{w_{it}}{r_{it}^\beta}\right) = A_i + a_{it} + u\left(C_{0i} e^{(1-\beta)\chi_{it}} \left(\frac{K_{it}^{1-\omega-\varpi}}{N_{it}^{1-\varpi}}\right)^\xi\right) \equiv U_i(a_{it}, \chi_{it}, K_{it}, N_{it}).$$

2.5 Migration decisions

Workers solve a forward-looking dynamic migration decision problem. We denote by V_{it} the value of being located in i at time t. V_{it} satisfies the Hamilton-Jacobi-Bellman (HJB) equation:

$$\rho V_{it} = U_i(a_{it}, \chi_{it}, K_{it}, N_{it}) + \mathcal{M}_i[V] + \frac{\mathbb{E}[d_t V_{it}]}{dt}, \tag{3}$$

where we used standard discrete choice results and denoted

$$\mathcal{M}_i[V] \equiv \mu \left\{\frac{1}{\nu} \log\left(\sum_j e^{\nu(V_{jt}-\tau_{ij})}\right) - V_{it}\right\}$$

the continuation value from migration. Finally, the last term in the worker's HJB equation represents the continuation value from changes in the aggregate state, where the notation d_t denotes the time increment due to changes in aggregates only and not due to individual migration.

Standard discrete choice results guarantee that migration shares are a function of the vector of values V, namely,

$$m_{ij}(V) = \frac{e^{\nu(V_j - \tau_{ij})}}{\sum_k e^{\nu(V_k - \tau_{ik})}}. \tag{4}$$

The population distribution evolves according to the Kolmogorov Forward (KF) equation

$$\frac{dN_{it}}{dt} = \mu \left(\sum_k m_{ki}(V_t) N_{kt} - N_{it} \right) \equiv \mu \left(\left(m^*(V_t) - \text{Id} \right) N_t \right)_i \tag{5}$$

In equation (5), m denotes the matrix of migration shares $m_{ij}(V_t)$. m^* denotes the matrix transpose of the matrix m. We also denote by $M^*(V) = \mu \left(m^*(V) - \text{Id} \right.$ a matrix that collects migration shares and the identity matrix, so that (5) becomes, in matrix notation, $\frac{dN_t}{dt} = M^*(V)N_t$. We denote $M(V) = \mu(m(V) - \text{Id}))$ the transpose of $M^*(V)$ for future reference.

2.6 Investment decisions

Capitalists solve a forward-looking dynamic investment decision problem. We denote $\mathcal{P}_{it}(K, b)$ the value of being located in i at time t and holding K units of local capital together with b units of bonds. $\mathcal{P}_{it}(K, b)$ satisfies the HJB equation:

$$\rho \mathcal{P}_{it}(K, b) = \max_{I,C} C + \left(\overline{R}_t b + R_{K,it} K + \theta_{it} - c_i(I/K)K - C \right) \frac{\partial \mathcal{P}_{it}}{\partial b} + \left(I - \Delta_{it} K \right) \frac{\partial \mathcal{P}_{it}}{\partial K} + \frac{\mathbb{E}_t[d_t \mathcal{P}_{it}]}{dt} \tag{6}$$

The first term in the capitalist HJB is the flow utility from consumption. The second term is the continuation value from net savings. Net savings are given by returns on bonds and capital, proceeds from the land-holding mutual fund, minus expenditures on investment adjustment costs and consumption. Net savings are valued at the marginal value $\frac{\partial \mathcal{P}_{it}}{\partial b}$. The third term represents the continuation value from net investment, namely, gross investment minus depreciation multiplied by the marginal value of capital $\frac{\partial \mathcal{P}_{it}}{\partial K}$. The final term in the capitalists' HJB is the continuation value from changes in the aggregate state.

We show in Appendix A.2 that $\mathcal{P}_{it}(K, b) = Q_{it}K + b + \mathcal{T}_{it}$, where $\mathcal{T}_{it}$ is the present value of transfers from the mutual fund, and Q_{it} satisfies

$$\rho Q_{it} = R_i(\chi_{it}, K_{it}, N_{it}) + \frac{c_{i0} Q_{it}^{1+\zeta}}{1+\zeta} - \delta_{it} Q_{it} + \frac{\mathbb{E}_t[\partial_t Q_{it}]}{dt}. \tag{7}$$

The investment policy of capitalists then satisfies $I_{it}^* = c_{i0} Q_{it}^\zeta K_{it}$. The law of motion of capital in every

location becomes

$$\frac{dK_{it}}{dt} = (c_{i0}Q_{it}^{\zeta} - \Delta_{it})K_{it}. \tag{8}$$

2.7 Steady-state

In steady-state at baseline temperatures, $\epsilon = 0$. All time derivatives are equal to zero. The HJB equation of workers (3) becomes:

$$\rho V_i^{SS} = U_i(0, 0, K_i^{SS}, N_i^{SS}) + \mathcal{M}_i[V^{SS}]. \tag{9}$$

The HJB of capitalists and (7) becomes

$$\rho Q_i^{SS} = R_i(0, K_i^{SS}, N_i^{SS}) - \frac{c_{i0}(Q_i^{SS})^{1+\zeta}}{1+\zeta}, \tag{10}$$

and the steady-state population distribution $N^{SS} = \{N_i^{SS}\}_i$ satisfies

$$0 = M^*(V^{SS})N^{SS}. \tag{11}$$

The steady-state capital distribution $K^{SS} = \{K_i^{SS}\}_i$ is such that the capital stock remains stable in every location, namely,

$$0 = c_{i0}(Q_i^{SS})^{\zeta} - \Delta_i. \tag{12}$$

Appendix C describes a simple algorithm to solve for the steady-state that leverages equations (9)-(12).

3 The Master Equation, the FAME, and transitional dynamics

3.1 Strategy

Our economy is a dynamic general equilibrium economy in which the distributions of workers $N_t = \{N_{it}\}_i$ and capital $K_t = \{K_{it}\}_i$ are aggregate state variables that determine local prices. The distribution of workers and capital evolves slowly according to the laws of motions (5) and (8). These laws of motion in turn depend on the values of workers given by the HJB equations (3) and (7).

Solving for this dynamic fixed point is challenging in our high-dimensional environment with over 3,000 counties. We make progress by leveraging the 'Master Equation' representation of the economy developed in Bilal (2021).

The Master Equation approach is structured in two steps. In the first step, we merge the individual decision problems with the laws of motion of the population and capital distributions into a single Bellman

equation: the Master Equation. The Master Equation is a state-space representation of the equilibrium. The second step consists in taking a local perturbation of the Master Equation in the scale parameter ϵ around a steady-state of the economy. The key insight from the local perturbation is to simplify the dynamic fixed point to a set of simple and standard Bellman equations that we solve rapidly with entirely standard techniques. For clarity, we present a self-contained description of our approach that closely follows the steps in Bilal (2021).

3.2 The Master Equation

We start with the Master Equation for workers. We combine the HJB equation (3) with the laws of motion (5) and (8) with a simple change of variables. We index value functions by the population and capital distributions instead of calendar time alone. The core idea is that the population and capital distributions are no more than large-dimensional state variables from the perspective of any given worker. Of course, we need to keep calendar time as a separate index because of climate change embedded in global mean temperatures T_t^D.

Specifically, we change variables by writing $V_{it} = V_{it}(z_t, N_t, K_t)$ and $Q_{it} = Q_{it}(z_t, N_t, K_t)$, where now the time subscript t only captures dependence on deterministic temperature.[7] Recall that $N_t = \{N_{it}\}_i$ denotes the vector of population across locations at time t, and $K_t = \{K_{it}\}_i$ similarly denotes the capital distribution.

Using this change of variables, we use the chain rule to express the continuation value from changes in aggregate states as:

$$\mathbb{E}_{it}\left[\frac{d_t V_{it}}{dt}\right] = \underbrace{\frac{\partial V_{it}}{\partial t}}_{\substack{\text{change in } T_t^D}} + \underbrace{\mathcal{A}_\epsilon(z)[V_{it}]}_{\substack{\text{change in } z_t: \\ \text{continuation value}}} + \underbrace{\sum_j \frac{\partial V_{it}}{\partial N_j}\frac{dN_{jt}}{dt}}_{\substack{\text{change in } N_t: \\ \text{chain rule}}} + \underbrace{\sum_j \frac{\partial V_{it}}{\partial K_j}\frac{dK_{jt}}{dt}}_{\substack{\text{change in } K_t: \\ \text{chain rule}}}, \tag{13}$$

where $\mathcal{A}_\epsilon(z)$ is an operator that embeds the continuation value arising from natural climate variability. For instance, if z_t follows a continuous-time AR(1) process $dz_t = -\theta z_t + \sigma dW_t$, the operator $\mathcal{A}_\epsilon(z)$ is given by $\mathcal{A}_\epsilon(z)[V] = -\theta z\epsilon\frac{\partial V}{\partial z} + \frac{\sigma^2 \epsilon^2}{2}\frac{\partial^2 V}{\partial z^2}$.

The last two components encode how the value of workers changes with the population and capital distributions across locations. When workers reallocate across locations in equilibrium, or when the distribution of capital shifts in equilibrium, the distribution of local wages, building rental rates, and capital rental rates change. These changes in these three distributions of prices affect residents of location i.

We then use the laws of motion of the population and capital distributions (5) and (8) to express the

---

[7]If the evolution of temperature was determined by current temperature and the evolution of the economy through its emissions, as in a integrated assessment models of the world economy, we would simply add temperature as a state variable and eliminate time dependence in the value function altogether.

time change of population and capital in (13). After this substitution into the continuation value (13) and into the HJB (3), we obtain the Master Equation for workers:[8]

$$
\rho V_{it}(z, N, K) = \underbrace{U_i \Big(a_i(\epsilon(z + T_t^D)), \chi_i(\epsilon(z + T_t^D)), K_i, N_i \Big)}_{\text{flow payoff}} + \underbrace{\mathcal{M}_i[V]}_{\substack{\text{continuation value} \\ \text{from own migration}}} \tag{14}
$$

$$
+ \underbrace{\sum_j \frac{\partial V_{it}}{\partial N_j} \left(M^*(V) N_t \right)_j + \sum_j \frac{\partial V_{it}}{\partial K_j} \left(c_{j0} Q_{jt}^\zeta - \Delta_j - \delta_j(\epsilon(z + T_t^D)) \right) K_j + \mathcal{A}_\epsilon(z)[V_{it}] + \frac{\partial V_i}{\partial t}}_{\text{continuation values from aggregate changes}}.
$$

Note that the Master Equation for workers depends on the value of capitalists Q because the latter affects investment, capital accumulation, prices, and, ultimately, worker welfare.

A similar logic delivers the Master Equation for capitalists, which is given by

$$
\rho Q_{it}(z, N, K) = \underbrace{R_i \left(\chi_i(\epsilon(z + T_t^D)), K_i, N_i \right)}_{\text{flow payoff}} + \underbrace{\frac{c_{i0} Q_i^{1+\zeta}}{1+\zeta} - \left(\Delta_i + \delta_i(\epsilon(z + T_t^D)) \right) Q_{it}}_{\text{continuation values from own investment}} \tag{15}
$$

$$
+ \underbrace{\sum_j \frac{\partial Q_{it}}{\partial N_j} \left(M^*(V) N_t \right)_j + \sum_j \frac{\partial Q_{it}}{\partial K_j} \left(c_{j0} Q_{jt}^\zeta - \Delta_j - \delta_j(\epsilon(z + T_t^D)) \right) K_j + \mathcal{A}_\epsilon(z)[Q_{it}] + \frac{\partial Q_{it}}{\partial t}}_{\text{continuation values from aggregate changes}}.
$$

Our equilibrium definition is standard and therefore omitted. The main advantage of the Master Equations (14)-(15) is that they provide a parsimonious representation of the general equilibrium of the economy. The derivations above prove our first result.

Proposition 1. *(Equilibrium)*
A solution (V, Q) to the Master Equations (14)-(15) together with a solution to the population and capital distributions $\{N_t, K_t\}_t$ to the KF equations (4) and (8) is an equilibrium of our economy.

3.3 The FAME

Despite providing a parsimonious representation of the equilibrium, the nonlinear Master Equations (14)-(15) are challenging to solve numerically because they depend on large-dimensional distributions. Existing numerical techniques would rapidly run into the curse of dimensionality. Instead, we use an analytic approach to gain economic insights and substantially simplify the computational burden. Following Bilal (2021), we use a local perturbation technique. Namely, we seek a local solution to the Master Equations (14)-(15) when the scale parameter ϵ is small enough. That is, we solve the First-order Approximation to the Master Equations (FAME).

The FAME is a first-order Taylor expansion of the Master Equations (14)-(15) in ϵ around the initial steady-state. We consider distributions and shocks that are close enough to steady-state. Namely, denote

---

[8]We omit the full dependence of the value function and its derivatives on (K, N, t, ϵ) on the right-hand-side for brevity.

$N = N^{SS} + \epsilon n$ and $K = K^{SS} + \epsilon k$, where the vectors n, k denote scaled deviations of the population and capital distributions from steady-state.

We then seek a solution of the form

$$
\begin{aligned}
V_{it}(z, N^{SS} + \epsilon n, K^{SS} + \epsilon k) &= V_i^{SS} + \epsilon \left\{ \sum_j v_{ij}^N n_j + \sum_j v_{ij}^K k_j + v_i^Z z + v_{it}^T \right\} + \mathcal{O}(\epsilon^2), \\
Q_{it}(z, N^{SS} + \epsilon n, K^{SS} + \epsilon k) &= Q_i^{SS} + \epsilon \left\{ \sum_j q_{ij}^N n_j + \sum_j q_{ij}^K k_j + q_i^Z z + q_{it}^T \right\} + \mathcal{O}(\epsilon^2).
\end{aligned}
\tag{16}
$$

The additive separability follows from the first-order Taylor expansion in ϵ.

Thus, instead of seeking full functions V, Q as solutions to the Master Equations, the first-order approach lets us seek a restricted number of coefficients: the directional derivatives $v_{ij}^N, v_{ij}^K, v_i^Z, v_{it}^T$ of the value function with respect to the population and capital distributions, temperature shocks and temperature trends. We call these derivatives the 'impulse values' following Bilal (2021). We substitute the first-order Taylor expansions (16) into the Master Equations (14)-(15) and obtain a set of restrictions on these directional derivatives: the FAME. These restrictions constitute our second key set of results.

Proposition 2. *(Deterministic FAME)*
The matrices v^N, v^K, q^N, q^K satisfy the generalized Sylvester matrix equation:

$$
\rho \mathrm{v}^d = \mathrm{D}^d + \mathrm{M}\mathrm{v}^d + \mathrm{v}^d \mathrm{M}^* + \mathrm{v}^d \mathrm{P}^d \mathrm{v}^d, \quad \mathrm{v}^d \equiv \begin{pmatrix} v^N & v^K \\ q^N & q^K \end{pmatrix},
$$

where M denotes the steady-state matrix $M(V^{SS})$, and we defined the following $2\mathcal{I} \times 2\mathcal{I}$ matrices:

$$
\mathrm{D}^d = \begin{pmatrix} -D_{UN} & D_{UK} \\ -D_{RN} & D_{RK} \end{pmatrix}, \quad \mathrm{M} = \begin{pmatrix} M & 0 \\ 0 & 0 \end{pmatrix}, \quad \mathrm{P}^d = \begin{pmatrix} G & 0 \\ 0 & D_{IQ} \end{pmatrix},
$$

and where

$$
\begin{aligned}
D_{UN} &= \xi(1-\varpi)\mathbf{diag}\left(u'(C_i^{SS})C_i^{SS}/N_i^{SS}\right) & D_{UK} &= \xi(1-\omega-\varpi)\mathbf{diag}\left(u'(C_i^{SS})C_i^{SS}/K_i^{SS}\right) \\
D_{RK} &= -\phi\mathbf{diag}\left(R_i^{SS}/K_i^{SS}\right) & D_{RN} &= -\psi\mathbf{diag}\left(R_i^{SS}/N_i^{SS}\right) \\
G &= \mu\nu\left(\mathbf{diag}(N^{SS}) - m^*\mathbf{diag}(N^{SS})m\right) & D_{IQ} &= \zeta\mathbf{diag}\left(K_i^{SS}c_{i0}(Q_i^{SS})^{\zeta-1}\right).
\end{aligned}
$$

Proof. See Appendix B. □

The deterministic FAME in Proposition 2 is a Bellman equation that is satisfied by the deterministic impulse values v^N, v^K, q^N, q^K. This Bellman equation takes the form of a nonlinear Sylvester matrix

equation.[9]

The right-hand-side of the FAME has four components. Each one encodes a particular force that affects how the value of workers and capitalists in location i changes in equilibrium when an additional worker enters location j or an additional unit of capital is added in location j.

The first component in the deterministic FAME is the direct price impact matrix D^d. When population and capital distributions change, prices also change. The movement in prices affects the flow payoff of workers and capitalists. The upper left block of the price impact matrix D^d, D_{UN}, encapsulates how changes in the population distribution affect workers in location i. The combination of parameters $\xi(1-\varpi)$ summarize the effect on real wages. The real wage effect is then converted into utility units by the diagonal marginal utility matrix $\mathbf{diag}\left(u'(C_i^{SS})C_i^{SS}/N_i^{SS}\right)$. The upper right block of the impact matrix D^d, D_{UK}, encapsulates how changes in the capital distribution affect workers in location i through their effect on real wages. The lower half of the price impact matrix D^d, $(-D_{RN} \ D_{RK})$, similarly reflects how changes in the population and capital distributions affect the return on capital.

The second component in the deterministic FAME, $\mathrm{M}v^d$, encodes a partial equilibrium force. When the value of locating in a particular region changes because of population and capital flows, the migration decisions of workers change. The second component of the FAME encapsulates the option value of migration. Crucially, the FAME reveals that workers only need to evaluate this option value using their steady-state migration matrix M. This property arises because of the envelope condition: migration decisions are already optimal before the economy moves out of steady-state.

The third component in the deterministic FAME, $v^d\mathrm{M}^*$, represents a first general equilibrium force. When contemplating the effect of an additional worker in location j on the economy, workers and capitalists in location i expect this additional worker in location j to behave just as any other worker. In particular, the worker in location j will migrate going forward. Keeping track of where this worker goes matters to project the economy forward in time and evaluate how the population distribution will evolve. The FAME shows that this expectation is summarized by the steady-state migration matrix M.[10] Once more, only the steady-state transition matrix M matters because changes in migration patterns envelope out. The (augmented) steady-state matrix M^* right-multiplies the deterministic impulse value because it represents the effect of an additional worker in location j on the value of workers and capitalists in location i.

The fourth component in the deterministic FAME, $v^d\mathrm{P}^d v^d$, encodes a second general equilibrium force. It represents how workers and capitalists in location i value changes in the law of motion of the population and capital distributions that arise because of an additional worker or capital unit in location j. Why would the law of motion change? An additional worker or capital unit in location j affects prices. Because prices change, all workers and capitalists change their migration and investment behavior. This change

---

[9]A standard Sylvester matrix equation is a matrix equation in an unknown matrix X such that $AX + XB + C = 0$.

[10]The corresponding component for capital drops out because there is no gross capital growth in steady-state in any location.

in migration and investment behavior affects the law of motion of the distribution to first order through the matrix $\mathrm{P}^d \mathrm{v}^d$. Ultimately, this change affects any given worker and capitalist after converting it into utility units using the deterministic impulse value v^d.

Proposition 2 highlights the first two key properties of the FAME. First, the deterministic FAME is a standard Bellman equation in finite dimension. The dimensionality of the impulse value v^d is simply $(2\mathcal{I})^2$, instead of being infinite-dimensional like the nonlinear Master Equations (14)-(15). This drastic simplification stems from the local perturbation. Workers and capitalists in location i need only consider isolated impulses in the population and capital distribution (N_t, K_t) at any other possible location j: any pairwise impulses would lead to a second-order deviation in the value function.

Second, all the objects entering in the FAME are steady-state objects with closed form expressions. This property is a consequence from the analytic nature of the perturbation. This observation implies that, once the nonlinear steady-state of the model is known, no additional calculation is needed to set up the FAME.

With the deterministic FAME at hand, we solve for the trend FAME. Namely, for the values of v^T and q^T in equations (16). This is important since we capture direct changes in temperature through these terms. The stochastic FAME (v^Z and q^Z), where we could capture the direct effect of climate variability, follows a similar equation that we report in Appendix B.

Proposition 3. *(Trend FAME)*
The matrices v_t^T, q_t^T satisfy the Ordinary Differential Equation system:

$$\rho \mathrm{v}_t^T = D_t^T + \mathrm{M}\mathrm{v}_t^T + \frac{\partial \mathrm{v}_t^T}{\partial t} + \mathrm{v}^d \mathrm{P}^d \mathrm{v}_t^T, \quad \mathrm{v}_t^T \equiv \begin{pmatrix} v_t^T \\ q_t^T \end{pmatrix},$$

where we defined the $2\mathcal{I} \times 1$ vector

$$D_t^T = T_t^D \begin{pmatrix} D_{UT} - v^K D_{\Delta T} \\ -D_{QT} - q^K D_{\Delta T} \end{pmatrix},$$

and where $a_{i1} = a_i'(0)$, $\chi_{i1} = \chi_i'(0)$, $\delta_{i1} = \delta_i'(0)$, so that:

$$D_{UT} = \mathbf{vec}\Big(a_{i1} + u'(C_i^{SS})C_i^{SS}(1-\beta)\chi_{i1}\Big), \quad D_{\Delta T} = \mathbf{vec}\Big(K_i^{SS}\delta_{i1}\Big), \quad D_{QT} = \mathbf{vec}\Big(\delta_{i1}Q_i^{SS} - R_i^{SS}\chi_{i1}\Big).$$

Proof. See Appendix B. □

The structure of the trend FAME in Proposition 3 is similar to the deterministic FAME in Proposition 2. The first component D_t^T in the trend FAME is the direct climate impact. When global temperatures rise, climate damages intensify. The damage matrices D_{UT}, D_{QT} and $D_{\Delta T}$ capture these forces through the damage coefficients a_{i1}, χ_{i1}, and δ_{i1}. The deterministic impulse values v^K, q^K enter in the direct

climate impact because workers and capitalists value depreciation damages going forward through their effect on the law of motion of the capital distribution.

The second component $\mathrm{M}\mathrm{v}_t^T$ in the trend FAME encodes the partial equilibrium option value of migration. When the value of locating in a particular region changes because of climate damages, migration decisions of any given worker change according to the steady-state migration matrix M.

The third component $\frac{\partial v_t^T}{\partial t}$ in the trend FAME encodes how exogenous changes in global mean temperatures affect workers and capitalists.

The fourth component in the FAME, $\mathrm{v}^d\mathrm{P}^d\mathrm{v}_t^T$, encodes a general equilibrium force. It represents how workers and capitalists in location i value changes in the law of motion of the population and capital distributions that arise because of climate damages. These changes in the laws of motion are valued through the deterministic impulse value v^d.

Proposition 3 reveals the third key property of the FAME: block-recursivity. The deterministic FAME does not depend on the trend or stochastic FAMEs. One can solve for the deterministic FAME in a first step. In a second step, given the deterministic impulse value v^d, one solves for the trend and stochastic impulse values v^T and v^Z.

3.4 Transitional dynamics

With value functions and thus policy functions at hand from the FAME, we obtain the law of motion of population and capital across locations for a sequence of climate change shocks.

Proposition 4. *(Transitional dynamics)*
Given initial conditions n_0, k_0, the transitional dynamics in response to a sequence of shocks $\{z_t\}_t$ and $\{T_t^D\}_t$ are given by paths $\{n_t, k_t\}_t$ such that:

$$\frac{d}{dt}\begin{pmatrix} n_t \\ k_t \end{pmatrix} = (\mathrm{M}^* + \mathrm{P}^d)\begin{pmatrix} n_t \\ k_t \end{pmatrix} + \mathrm{P}^d(\mathrm{v}_t^T + z_t\mathrm{v}^Z) - (T_t^D + z_t)\begin{pmatrix} 0 \\ D_{\Delta T} \end{pmatrix}. \tag{17}$$

Proposition 4 strengthens the block-recursivity structure of the FAME since the FAME inherits the block-recursivity from the Master Equation. The FAME is the only fixed point that must be solved to determine individual behavior. There is no additional price or distributional fixed point to solve because these fixed points are merged into the Master Equation, and hence into the FAME. Given impulse values $\mathrm{v}^d, \mathrm{v}^T, \mathrm{v}^Z$, any counterfactual impulse response obtains from a single time iteration as per Proposition 4.

3.5 Welfare

Equipped with values and allocations in the FAME, we characterize the welfare effect of climate change. We denote by $\overline{V}_t = \sum_i N_i V_{it}$ utilitarian worker welfare, and by $d\overline{V}_t$ the change in utilitarian welfare

following climate change. This welfare metric does not include current preference shocks and is consistent with the interpretation in which preference shocks are experienced once and for all upon moving.[11]

Proposition 5. *(Worker welfare)*
The change in worker welfare in response to climate change can be decomposed according to

$$d\overline{V}_t = \underbrace{\mathbb{E}_N[\epsilon v_{it}^T]}_{direct\ impact} + \underbrace{\mathbb{C}\mathrm{ov}_N\left[V_i^{SS}, \widehat{n}_{it}\right]}_{value\ reallocation:\ PE} + \underbrace{\mathbb{C}\mathrm{ov}_N\left[\varepsilon_i^{vN}, \widehat{n}_{it}\right] + \mathbb{C}\mathrm{ov}_K\left[\varepsilon_i^{vK}, \widehat{k}_{it}\right]}_{elasticity\ reallocation:\ GE} + \underbrace{\mathbb{E}_K\left[\varepsilon_i^{vK}\right]\widehat{\overline{k}}_t}_{aggregate\ capital},$$

where

$$\varepsilon_i^{vN} = \mathbb{E}_N[v_{\bullet i}^N], \qquad \varepsilon_i^{vK} = \mathbb{E}_N[v_{\bullet i}^K], \qquad \widehat{n}_{it} = \frac{\epsilon n_{it}}{N_i^{SS}}, \qquad \widehat{k}_{it} = \frac{\epsilon k_{it}}{K_i^{SS}}, \qquad \widehat{\overline{k}}_t = \epsilon \sum_i k_{it},$$

and $\mathbb{E}_N, \mathbb{C}\mathrm{ov}_N, \mathbb{E}_K, \mathbb{C}\mathrm{ov}_K$ *denote expectations and covariances weighted by the steady-state population (N) or capital (K) distributions.*[12]

Proof. See Appendix B.6.1. ☐

We also show in Appendix B.6.2 that the change in consumption-equivalent welfare $d\omega_t$ is then related to the change in utilitarian welfare by

$$d\omega_t = \frac{\rho d\overline{V}_t}{\widetilde{V}},$$

where $\widetilde{V}_i$ satisfies the HJB $(\rho + \mu)\widetilde{V}_i = \rho(C_i^{SS})^{1-\gamma} + \mu \sum_j m_{ij}\widetilde{V}_j$ and is equal to 1 under log utility, $\gamma = 1$, and $\widetilde{V} = \sum_i N_i^{SS}\widetilde{V}_i$.

Proposition 5 reveals that aggregate welfare changes split into four components. The direct impact component $\mathbb{E}_N[\epsilon v_{it}^T]$ reflects the direct effect of climate change through the trend impulse value v_{it}^T.

The value reallocation component $\mathbb{C}\mathrm{ov}_N\left[V_i^{SS}, \widehat{n}_{it}\right]$ reflects a partial equilibrium force. Climate change generates net migration out of highly affected locations and towards locations that are less affected. This net migration generates welfare changes if destination locations are more valuable than origin locations. The covariance between population changes and local valuations summarizes this effect. Because of the first-order perturbation nature of the FAME, it suffices to use the steady-state valuations V_i^{SS} to evaluate whether climate-induced net migration is beneficial or harmful to the average worker.

The elasticity reallocation component $\mathbb{C}\mathrm{ov}_N\left[\varepsilon_i^{vN}, \widehat{n}_{it}\right] + \mathbb{C}\mathrm{ov}_K\left[\varepsilon_i^{vK}, \widehat{k}_{it}\right]$ reflects general equilibrium forces. Climate change leads to net population and capital flows. These flows affect local prices, which

---

[11]We also consider an alternative welfare metric that includes the distribution of preference shocks of current residents: $\mathcal{W}_{it} = \frac{1}{\nu}\log\left(\sum_j e^{\nu(V_{jt} - \tau_{ij})}\right)$. This metric is consistent with the interpretation in which preference shocks are permanently enjoyed until the next moving opportunity. In that case, we denote $\overline{\mathcal{W}}_t = \sum_i N_i \mathcal{W}_{it}$ utilitarian worker welfare, and by $d\overline{\mathcal{W}}_t$ welfare changes.

[12]When using the welfare metric $d\overline{\mathcal{W}}_t$, replace V_i^{SS} with $\mathcal{W}_i^{SS}$ in the value reallocation component.

feed back into worker welfare. The impact of local price movements is summarized by the deterministic impulse values v^N, v^K from the FAME, averaged into the elasticities $\varepsilon^{vN}, \varepsilon^{vK}$. Whether price movements affect welfare ultimately depends on the covariance between population and capital net flows on the one hand, and average impulse values $\varepsilon^{vN}, \varepsilon^{vK}$ on the other hand.

The aggregate capital component $\mathbb{E}_K\left[\varepsilon_i^{vK}\right]\widehat{\overline{k}}_t$ captures changes in the overall capital stock of the economy. If climate change leads to higher capital depreciation or declines in investment, the aggregate capital stock shrinks. This reduction affects workers through the average impulse value ε^{vK}.

Our counterfactuals in Section 6 explore the role of migration as an adaptation mechanism. The decomposition in Proposition 5 makes immediately evident that migration affects welfare through the partial equilibrium value reallocation component, the general equilibrium elasticity reallocation component, as well as possibly through the aggregate capital component. Note, however, that the direct impact component also depends on migration as evidenced by Proposition 3. The trend FAME v_t^T depends on migration through three channels: first, the steady-state migration share matrix M because of the option value of migration; second, the valuation of capital depreciation through v^K; third, changes in general equilibrium migration patterns through G.

Our key result is that the option value of migration is irrelevant for the direct impact of climate change. Indeed, Proposition 3 immediately implies that $E_N[v_t^T]$ satisfies the ODE

$$\rho E_N[v_t^T] = T_t^D \mathbb{E}_N[D_{UT} - v^K D_{\Delta T}] + 0 + \frac{\partial E_N[v_t^T]}{\partial t} + \mathbb{E}_N[v^d \mathrm{P}^d v_t^T]. \tag{18}$$

The option value of migration Mv_t^T drops out once aggregated across all workers in the economy. Algebraically, this result is a direct consequence of the determination of the steady-state population distribution in equation (11), namely, $E_N[Mv_t^T] = N'Mv_t = 0$.

Why is the option value of migration irrelevant for aggregate welfare? The intuition lies in an envelope argument. Prior to climate change, workers make privately optimal migration decisions. Once climate change occurs, workers adjust their migration decisions. But just as with any decision, the valuation of the climate change shock enters only through its direct effect on workers Mv_t^T. Prior to climate change, the marginal worker is already indifferent between their preferred and runner-up locations. Thus, there are no welfare gains from adjusting migration decisions in response to climate change.

Under the FAME, the direct effect Mv_t^T is then evaluated using steady-state migration decisions. But because the average worker does not migrate on net in steady-state—there are gross migration flows but no net migration flows—the direct effect Mv_t^T averages to zero across all workers. This result generalizes those in Deryugina and Hsiang (2017) to a setting with heterogeneous workers who make dynamic decisions.[13]

---

[13]Our irrelevance result holds exactly because the FAME is a first-order perturbation, and so the envelope condition applies exactly. In a global solution, higher-order effects may become relevant.

Of course, the option value of migration may still matter indirectly for the direct impact $E_N[v_t^T]$ in equation (18) through either the valuation of capital depreciation v^K or through changes in general equilibrium migration patterns through the term $\mathrm{P}^d v_t^T$. Our quantitative exercises in Section 6 unpack the relative importance of these forces.

3.6 Implementation

Proposition 2 indicates a straightforward algorithm to compute the deterministic impulse value. Indeed, all the known inputs into the deterministic FAME can be directly constructed given steady-state objects. Thus, given steady-state objects, we directly construct the $2\mathcal{I} \times 2\mathcal{I}$ matrices D_d, M and P^d. We then seek a $2\mathcal{I} \times 2\mathcal{I}$ matrix v^d that satisfies the nonlinear Sylvester matrix equation

$$0 = \mathrm{D}_d + (\mathrm{M} - \rho \mathrm{Id}) \mathrm{v}^d + \mathrm{v}^d (\mathrm{M}^* + \mathrm{P}^d \mathrm{v}^d).$$

Following Bilal (2021), we use a simple iterative algorithm to solve for v^d. Given a guess v_n^d at step n, we solve for v_{n+1}^d as follows:

$$0 = \mathrm{D}_d + (\mathrm{M} - \rho \mathrm{Id}) \mathrm{v}_{n+1}^d + \mathrm{v}_{n+1}^d (\mathrm{M}^* + \mathrm{P}^d \mathrm{v}_n^d) \implies \mathrm{v}_{n+1}^d = \texttt{sylvester}\Big(\mathrm{M} - \rho \mathrm{Id}, \mathrm{M}^* + \mathrm{P}^d \mathrm{v}_n^d, \mathrm{D}_d \Big),$$

where $\texttt{sylvester}(A, B, C)$ denotes the solution X of the Sylvester equation $AX + XB + C = 0$. Given v_n^d, standard numerical packages solve efficiently for v_{n+1}^d as the root of a standard Sylvester equation.[14] Why choose to use the guess from last iteration v_n^d in this specific part of the Sylvester equation? The intuition is to use the guess from last iteration v_n^d where a given worker considers the valuations of other individuals, and solve for the valuation of the current individual v_{n+1}^d in the current step.

Once we have solved for the deterministic impulse value v^d, we solve for the trend impulse value leveraging Proposition 3 in two steps. In the first step, we solve for the long-run trend impulse value. When time t is large enough, temperatures do not change anymore. The economy has then reached the new steady-state, and $\frac{\partial \mathrm{v}^T}{\partial t} = 0$. Hence, we specify a large enough time $t = \bar{t}$ where the time derivative is zero, and where we use Proposition 3 to solve for $\mathrm{v}_{\bar{t}}^T$. Specifically, $\mathrm{v}_{\bar{t}}^T = (\rho \mathrm{Id} - (\mathrm{M} + \mathrm{v}^d \mathrm{P}^d)))^{-1} \mathrm{D}_{\bar{t}}^T$. The solution $\mathrm{v}_{\bar{t}}^T$ is our terminal condition.

In the second step, we iterate backward in time from the terminal condition $\mathrm{v}_{\bar{t}}^T$. We construct the $2\mathcal{I} \times 1$ vector D^T for each time t. Given a time step dt, we construct a solution v_t^T to the ODE system in Proposition 3 given $\mathrm{v}_{t+\mathrm{dt}}^T$ by iterating backward in time:

$$\mathrm{v}_t^T = \big(\mathrm{Id} + \mathrm{dt}(\rho \mathrm{Id} - (\mathrm{M} + \mathrm{v}^d \mathrm{P}^d)) \big)^{-1} \big(\mathrm{dt}\, \mathrm{D}_t^T + \mathrm{v}_{t+\mathrm{dt}}^T \big).$$

Once we have solved for the deterministic and trend impulse values, we compute any impulse response to

---

[14]For instance, Matlab has a built-in $\texttt{sylvester.m}$ function.

a shock or initial conditions with a simple forward iteration using Proposition 4. Having established an efficient solution method, we turn to our reduced-form estimates and estimation strategy.

4   Reduced-form impact of natural disasters

In order to quantify our model in a way that accounts well for the economic impact of climate change, we start by estimating the reduced-form impact that climate change has had on economic outcomes. In the next section we use these results to estimate the climate damage functions, as well as the mobility and investment elasticities.

4.1   Data

We combine data of two types. First, we use economic data from several sources by county and year. We collect data on population, income per capita, wages and employment from the Bureau of Economic Analysis. We obtain investment data at 5-year intervals from the Census of Manufactures. These data span the years 1960 to 2019. We provide more details in Appendix G.1.

Second, we use weather data. We obtain daily information on surface temperature, windspeed, and precipitation for a raster at the $0.5°$ by $0.5°$ since 1901 from the inputs to the Inter-Sectoral Impact Model Intercomparison Project (ISMIP). This information consists of reanalysis data: it combines historical station-level weather measurements with a climate model to produce high-resolution weather information. We convert this information into a dataset that tracks annual extremes for every county and year in the U.S. We provide more details in Appendix G.2.

We seek to capture the impact of extreme weather events. To that end, we construct indicator variables that capture whether local weather realizations are above a pre-specified threshold. Specifically, we first consider weather variables X_{it} for county i at time t in the following list: (i) maximum daily windspeed in the year, (ii) maximum daily precipitation in the year, and (iii) fraction of days with temperature above the 95th percentile of the national annual mean temperature distribution in 1901-1910. We provide more details in Appendix G.3.

Our weather variables are designed to capture salient features of (i-ii) storms and flooding, which we combine into 'storms' and (iii) heat waves. Of course, the physical processes leading to and defining such events are necessarily more complex than the specific metrics available in large-scale datasets covering the entire U.S. for over a century. For our purposes, it only matters that these variables correlate strongly enough with actual storms, floods, and heat waves. Ultimately, the impact of our weather-related variables on economic activity determines climate damages regardless of their specific interpretation. We refer to our variables as storms and heat waves for expositional simplicity but acknowledge that our variables necessarily are a stylized measurement of the underlying phenomena.[15]

---

[15]Our measures also have the advantage of being objective physical measures, rather than human-made reports of storms

Figure 1: Global mean temperature over time.
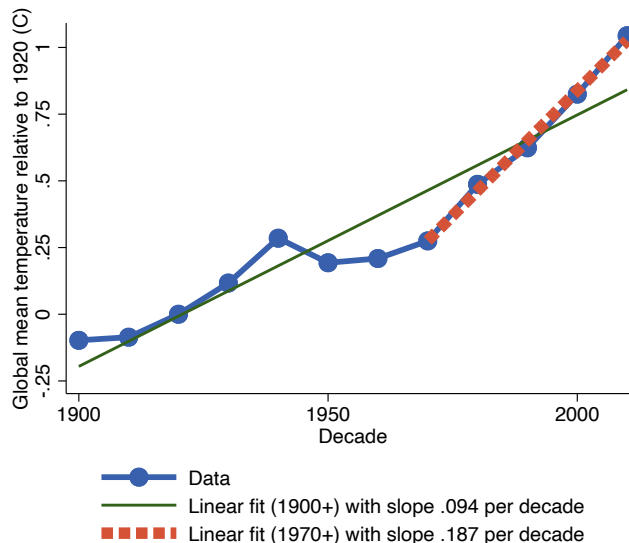
Different locations may be differentially adapted to natural disasters. To capture this adaptation and not overstate damages, we residualize our three weather variables X_{it} before constructing the indicator of extreme realizations. Therefore, we capture storm and heat wave realizations that are particularly severe relative to county-specific and annual conditions. Specifically, we strip out county and year fixed effects by estimating the linear regression:

$$X_{it} = \alpha_i + \beta_t + \hat{X}_{it}, \quad \mathbb{E}_i[\hat{X}_{it}] = \mathbb{E}_t[\hat{X}_{it}] = 0.$$

We then use the estimated residual $\hat{X}_{it}$ to construct our indicator of extreme value for $\hat{X}_{it}$:

$$D_{it} = \mathbf{1}[\hat{X}_{it} \geq \mathrm{p}(\hat{X})],$$

where $\mathrm{p}(\hat{X})$ denotes a given percentile of $\hat{X}_{it}$ across all counties i and years t. We choose realizations above the 99$^{\text{th}}$ percentile for windspeed and precipitation. This choice is guided by meteorological estimates of wind and concentrated precipitation measures that lead to property damages. It also coincides with the threshold at which we detect significant economic damages. We finally define our storm indicator as $D_{it}^{\text{storm}} = \max\{D_{it}^{\text{windspeed}}, D_{it}^{\text{precipitation}}\}$. A similar logic leads us to choose realizations above the 95$^{\text{th}}$ percentile for heat waves. We provide more details in Appendix G.3.[16]

4.2 Trends in natural disasters

We start by documenting salient trends in natural disasters over the course of the 20$^{\text{th}}$ century for the U.S. Figure 1 first shows the well-known fact that global mean temperatures have risen by over 1°C since

---

or floods that are likely to be endogenous to economic activity or population density.

[16]We also choose realizations below the 5$^{\text{th}}$ percentile for cold waves when we introduce them in Appendix D.1.

1900. The rate of warming has accelerated in the last decades, reaching nearly 0.2°C by decade.

Figure 2 presents a binned scatterplot of the relationship between global mean temperature and the annual probability of a 1-in-50-years storm and a 1-in-20-years heat wave.[17] We start with severe storms which occur every 50 years on average in the middle of the century according to our definition. The frequency of severe storms, presented in panel (a), rises substantially and approximately linearly with global mean temperatures across the U.S., consistently with the conclusions of the IPCC (2022).

Panel (a) reveals that the frequency of severe storms rises particularly fast in coastal counties—counties that have a coast along the Atlantic or Pacific oceans. A warming of 1°C over the course of the 20th century implies that the frequency of severe storms more than quadruples in coastal counties, from less than 2% to nearly 8%. These probabilities imply that severe storms used to occur less than every 50 years at pre-industrial temperatures in coastal counties. They now occur every 12 years. If global mean temperatures increase by 4°C by 2100 as in the business-as-usual scenario, severe storms would occur every 3 years in coastal counties. In contrast, the frequency of severe storms rises only modestly in inland areas—which we define as any county that does not have a coast along the Atlantic or Pacific oceans.

The frequency of heat waves, presented in panel (b) of Figure 2, also rises markedly as global temperatures rise, consistently with the conclusions from the IPCC (2022). We split our analysis between warm counties that have above-median average annual temperatures, and cold counties that have below-median average annual temperatures. We find that a heat wave that occurred every 20 years on average at 1920 global temperatures occurs every 5 years on average in 2023 in warm counties.[18] If global mean temperatures increase by 4°C by 2100 as in the business-as-usual scenario, a heat wave that happened only every 20 years in 1920 would happen every 2 years by 2100. By contrast, the frequency of heat waves in cold counties remains largely constant and close to zero.[19]

Which locations experience more natural disasters? Figure 2 indicates that coastal and warm counties have been more exposed in the last decades. We map out the detailed geography of exposure in Figure 3. The South-East Atlantic coast is particularly exposed to storms. For instance, counties in Texas, Louisiana, Florida, Georgia, North Carolina, and Virginia have experienced at least 3 severe storms since 1990. However, inland counties in states such as Nebraska and New York have also experienced several severe storms. Heat waves are prevalent across the South of the U.S. Some counties in Florida, Louisiana, Texas, Kansas, New Mexico, and Arizona are among the most exposed, with over 3 heat waves since 1990.

---

[17] We focus on observations post-1920 to have precisely one century of data.

[18] The prevalence of extreme heat is subject to important natural variability. For instance, the second square from the left corresponds to Dust Bowl years.

[19] We also show that the frequency of cold waves declines markedly with global temperature in Figure 13, Appendix D.1.

Figure 2: Natural disasters and global mean temperature.

(a) 1-in-50-years storm

(b) 1-in-20-years heat wave
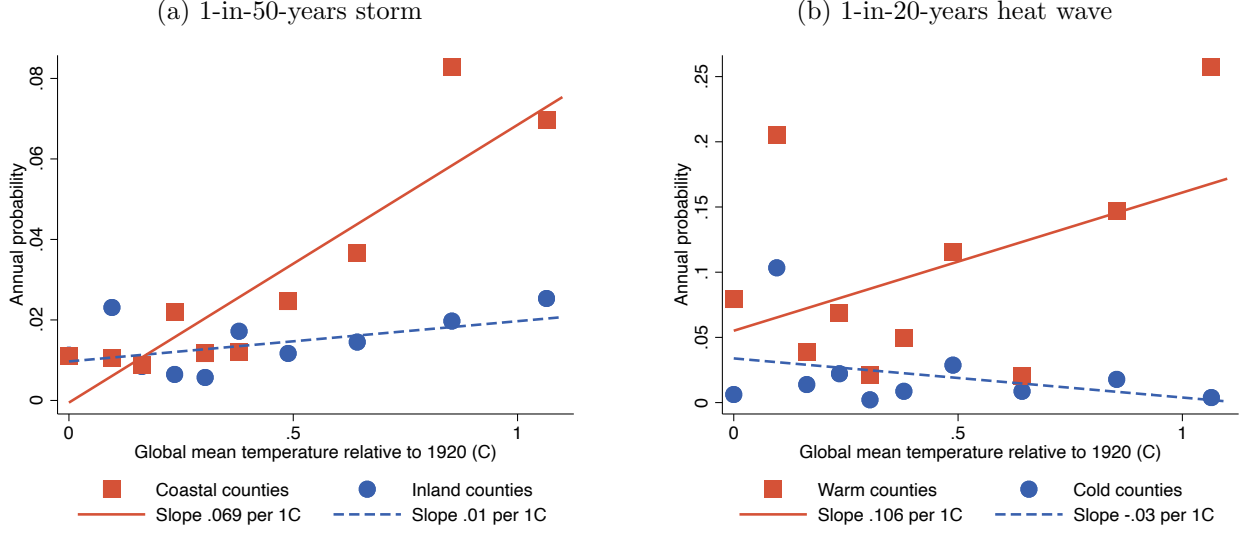
4.3 Event study design

The next step is to estimate the effect of a given natural disaster on economic activity. We use a standard distributed lag specification given by

$$y_{it} = \alpha_i + \beta_t + \sum_{h=-A}^{B} \gamma_h D_{i,t-h} + \gamma_{-A-1}\bar{D}_{i,t,-A-1} + \gamma_{B+1}\bar{D}_{i,t,B+1} + \delta_{S(i),t} + W_{it}\eta' + \varepsilon_{it}, \quad (19)$$

where i denotes counties and t denotes calendar years. y_{it} denotes the logged outcome of interest: income per capita, wages, employment, population, or investment. α_i is a county fixed effect, β_t is a year fixed effect. $D_{i,t-h}$ is our indicator that an extreme event occurred h years before calendar year t in county i. We include individual horizons h up to $A = 5$ years prior to and $B = 10$ years after the event. We also control for the average effect before A and after B: $\bar{D}_{i,t,-A-1} = \sum_{h \leq -A-1} D_{i,t-h}$, and $\bar{D}_{i,t,B+1} = \sum_{h \leq B+1} D_{i,t-h}$. $\delta_{S(i),t}$ denotes a set of trends by state, local mean temperature decile, local maximum daily windspeed and maximum precipitation deciles, population decile, and income per capita decile. W_{it} denotes a vector of time-varying county-specific controls that includes local government expenditures.[20] ε_{it} is a mean-zero residual. Our coefficients of interest are γ_h, the effect of an event h periods ago on outcomes today.

We focus on calendar years t after 2000. Restricting the data to focus on the post-2000 period lets us capture the most recent severity of extreme events in case it is time-varying. To the extent that not only the frequency but also the intensity of extreme events is projected to grow over time, our estimates represent a lower bound on expected damages going forward.[21]

We allow the effect of storms and temperature to differ depending on the characteristics of locations.

---

[20]Including or excluding government expenditures does not affect our conclusions.
[21]For storms, we restrict attention to counties that experience either zero or one event.

Figure 3: Natural disasters across counties.

(a) Storm counts since 1990   (b) Heat wave counts since 1990
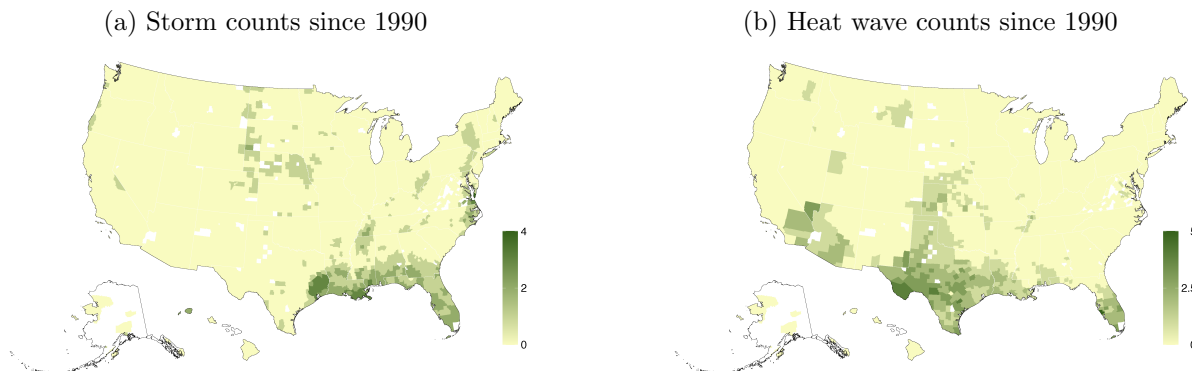
Note: Counties in white: missing data.

Namely, we allow the impact of storms to differ in coastal counties and inland counties. This split is natural given that severe storms on the coast may concur with coastal storm surges that worsen damages. In line with the literature that has found nonlinear effects of temperature on mortality and labor productivity (e.g. Deschênes and Greenstone, 2011 and Cruz and Rossi-Hansberg, 2023, respectively), we allow the effect of temperature to differ depending on the average temperature of a given location. We operationalize these ideas by running our analysis separately for coastal, inland, warm and cold counties as defined in Section 4.2.

Our identification condition is that treatment is randomly assigned conditional on our controls. Crucially, we include rich controls for location-specific trends $\delta_{S(i),t}$. These state-specific and county-group-specific trends absorb potentially important confounds to our exercise. For instance, demographic and income shifts have pushed high-income households to move to states such as Florida over the last 20 years. Florida also happens to be more exposed to severe storms and heat waves. As a result, omitting an adjustment to these background trends may lead to inferring that storms and heat waves increase income and employment.

Another concern for identification is whether the Stable Unit Treatment Value Assumption (SUTVA) is satisfied, namely that the control group remains unaffected by the treatment. This concern is valid given that in our model, untreated locations may respond to shocks in other regions because of general equilibrium effects. Thus, our empirical estimates may be biased by these general equilibrium effects. Our structural approach addresses this concern in two ways. First, we can explicitly inspect these general equilibrium effects inside our estimated model in Section 5. We find that these general equilibrium responses are small compared to the direct effect on treated locations. Second, we estimate our model by indirect inference: we replicate the same regression in the model and match the empirical coefficient—thus accounting for general equilibrium effects directly.

4.4 Results

We find that severe storms have a significant impact on economic activity in coastal counties. Figure 4 displays the impact of 1-in-50-year storms on six indicators of economic activity. Each panel shows year-by-year point estimates together with 95% confidence intervals.

Panel 4(a) shows that a 1-in-50-years storm lowers wages of employed workers by about 2.5% over 10 years. The effect for income per capita in panel 4(b), which accounts for self-employment and business income, is similar. Despite our rich set of controls, our estimated effects for income per capita display somewhat of an upward pre-trend. If we accounted for this differential trend, the estimated effect would be even larger. Panel 4(c) shows that population drops by 5% after 10 years in coastal counties that experience a severe storm. This decline in population is associated with a substantial reduction in employment in panel 4(d) which exceeds 8%. As with income per capita, and despite our rich controls, employment displays somewhat of an upward pre-trend. Again, if we accounted for it, our estimated effects would be even larger. Panel 4(e) reveals that investment booms after a severe storm, with a peak at 20% in the third year after the storm. To the extent that storms destroy capital, this positive investment response is natural given the need for reconstruction. Since our measure of investment only accounts for manufacturing investment, we reproduce our main result in Panel 4(f) where we rescale manufacturing investment by the manufacturing employment share in the same year. We find that this adjustment has virtually no effect on our results.[22]

Taken together, these results indicate that severe storms in coastal counties are well captured by a capital depreciation shock. Indeed, in our model—as in a standard Real Business Cycle model—a capital depreciation shock lowers wages and employment but increases investment, as the local economy rebuilds its capital stock. Key to this interpretation is the positive sign of the investment response. A negative investment response would, instead, suggest a negative productivity shock.[23]

Having established the effect of severe storms on economic activity, we turn to the impact of temperature. We start with the effect of heat waves on counties with temperatures above the median (warm counties). Figure 5 displays the impact of heat waves on the same six indicators of economic activity as for storms. Panel 5(a) shows that wages drop by 1% before recovering in a couple of years. Once we account for self-employment and business income, panel 5(b) reveals that income per capita displays a slightly larger response, but is more persistent over time. It takes 10 years for income per capita to fully recover. Population and employment both fall by 2.5% over the course of 10 years following a 1-in-20-years heat

---

[22]We also investigate the impact of severe storms on inland counties. We find no statistically significant or economically meaningful effect there. For completeness, we report these results in Figure 14 in Appendix D.2.

[23]The estimation above uses a selected sample of counties that experience only one windspeed and precipitation extreme event (one storm) in order to avoid confounding the cumulative effects of multiple storms. The reason is that, if the effects of multiple storms cumulate nonlinearly, controlling for past storms as in equation (19) may not be enough. We verify that our results are not sensitive to this choice. In Figure 15, Appendix D.2, we show that our main results continue to hold when we even consider counties that experience any number of storms. Although the response of population is somewhat muted in this larger sample, the responses of wages, income per capita, employment, and investment are all similar.

Figure 4: The impact of 1-in-50-years-storms on economic activity in coastal counties.
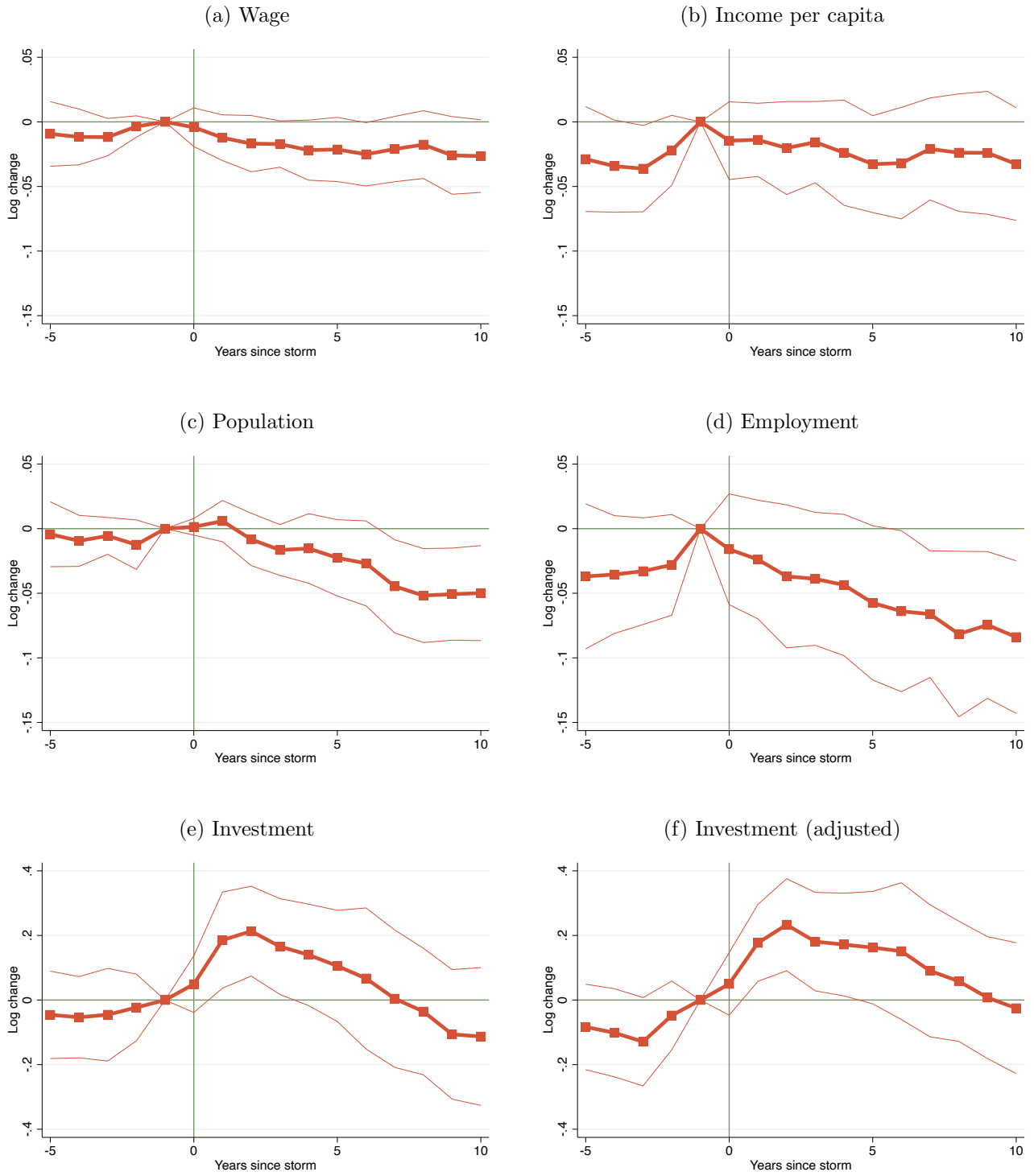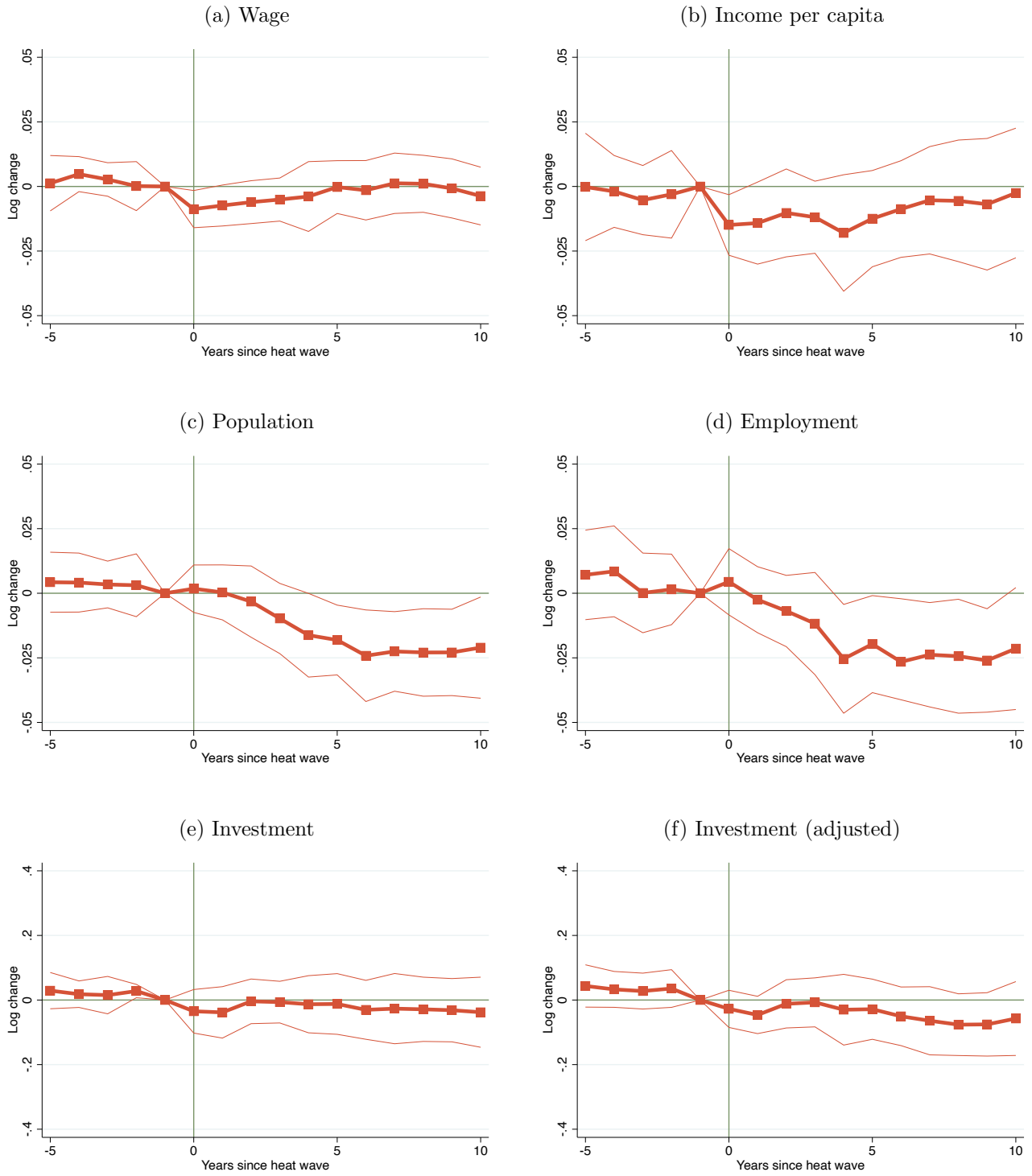
(a) Wage

(b) Income per capita

(c) Population

(d) Employment

(e) Investment

(f) Investment (adjusted)

Figure 5: The impact of 1-in-20-years heat waves on economic activity in warm counties.

(a) Wage

(b) Income per capita

(c) Population

(d) Employment

(e) Investment

(f) Investment (adjusted)

wave. Investment shows a moderate and negative response following a heat wave.

Together, these results suggest that heat waves in warm counties are well captured by a negative productivity shock. Crucially, the negative sign of the investment response allows us to differentiate the effect of a heat wave from the effect of a storm. Given the sizable population response in light of the moderate wage and income per capita response, these results indicate that heat waves may also be associated with a negative local amenity shock. Our structural estimation in Section 5 allows for both.[24]

We also estimate the impact of cold waves on economic activity. We do not detect statistically significant or economically consistent effects of cold waves in cold counties. We report them in Figure 16, Appendix D.3. Thus, we exclude cold waves from our main structural analysis in Sections 5 and 6. We report sensitivity analysis when we include cold waves, but their effect is quantitatively small relative to storms and heat.[25]

With estimates of the impact of extreme events on economic activity, we now turn to estimating the underlying damage functions.

5 Model Quantification

5.1 Baseline parameters

We start by determining baseline preference and technology parameters. Importantly, we estimate the two key migration and investment elasticities in Section 5.3 below. Throughout the rest of the paper, we interpret an interval $[t, t+1)$ as one year.

Preference parameters are determined as follows. We use a conservative time discount rate. Our value of $\rho = 0.03$ lies towards the high end of the range of values used in the climate change literature. Our baseline results should thus be seen as a lower bound on economic damages. We analyze the impact of different choices of the discount rate on our results in Section 6. We set the housing expenditure share for workers to the common value of $\beta = 0.3$. We set the risk-aversion parameter to $\gamma = 1$.

The next step is to determine the parameters governing migration decisions. We set $\mu = 2.30$ so that 90% of workers have the option to migrate within a year. We estimate bilateral migration costs τ_{ij} consistent with the empirical migration rate at baseline, as described in more detail below. Local amenities are estimated using the model inversion as described in the next section.

The parameters in the production function of goods and buildings are set to standard values. The share of commercial structures in goods production in the model includes both capital and physical structures in the data. Typical estimates put the first share at 0.3, and the second at 0.1. Together, we obtain

---

[24]Of course, heat waves may also have an effect in initially cold counties. However, there are too few heat waves in cold counties to let us reliably estimate these effects once we introduce our rich set of controls. Hence, we do not attempt to include these effects in our analysis.

[25]Similarly to heat, there are too few cold waves in warm counties to let us reliably estimate these effects once we introduce our rich set of controls. Hence, we do not attempt to include these effects in our analysis.

$\alpha = 0.4$. To obtain the share of labor ϖ in the production function of buildings, we measure the fraction of labor in the structures production sector x from the BEA input-output data. We obtain $x = 0.95$. Thus, we recover $\varpi = \frac{(1-\alpha)(1-x)}{\alpha x + (1-\alpha)\beta} = 0.05$ from equation (21). To obtain the share of land in the building production function ω, we use common estimates from the real estate literature. For a typical property, the value of land represents 20% of the property value, while the building value represents 80%. Hence, we set $\omega = 0.2$. Local productivities are the result of the model inversion, as described below.

The final set of parameters is related to investment choices. We impose a common capital depreciation rate of $\Delta_i = \Delta = 0.08$ for all counties at baseline. Of course, climate change affects the depreciation rate heterogeneously across locations. We estimate the investment elasticity and the local investment costs as described below.

5.2 Inversion of fundamentals

Our second step is to estimate time-invariant fundamentals for every location. Suppose for now that we have estimates of the migration elasticity ν and the investment elasticity ζ.

We use 2012 data for wages w_i, employment N_i, investment I_i, and migration flows $\mathbf{m}_{ij}$ for every pair of counties i, j. We also use county manufacturing employment shares π_i to adjust our measure of manufacturing investment $\tilde{I}_i = I_i/\pi_i$. We interpret 2012 as the initial stead-state of the economy. We use a recursive scheme to recover the time-invariant fundamentals in every location Z_i, A_i, c_{i0}, and τ_{ij}. The following proposition shows that, given the observed data, we can uniquely recover these fundamentals.

Proposition 6. *(Inversion of fundamentals)*
Given data $w_i, N_i, \tilde{I}_i, \mathbf{m}_{ij}$, there exists a unique set of vectors of fundamentals Z_i, A_i, c_{i0} and a unique symmetric migration cost matrix τ_{ij}.

Proof. See Appendix E. ☐

The proof of Proposition 6 is constructive and thus provides an algorithm to recover fundamentals. The proof extends standard static inversion arguments to our fully forward-looking dynamic setting. We can only recover symmetric migration costs because we invert them non-parametrically.[26]

5.3 Migration and investment elasticities

Our inversion argument relies on knowledge of the migration and investment elasticities ν, and ζ. We estimate those internally using our reduced-form estimates of the impact of extreme events on economic activity. Thus, we nest our inversion procedure in an outer loop in which we sample possible values for ν and ζ.

---

[26]Without symmetry, they are not separately identified from local amenities. If we imposed instead that migration costs depend on some distance metric, we could, of course, estimate this dependence flexibly.

Consistently with our reduced-form results, we assume that storms only generate a capital depreciation shock. Heat waves generate a simultaneous productivity and amenity shock. We assume that local amenities and local productivity respond proportionally to temperature shocks, such that $a_{i1}/\chi_{i1} = \eta$. The effect of heat waves remains heterogeneous across locations, but locations that experience larger productivity shocks due to heat waves also experience larger amenity shocks.

We then proceed by indirect inference. We draw triplets $\theta \equiv (\nu, \eta, \zeta)$.[27] For every triplet (ν, η, ζ), we first solve for the steady-state following Section 2.7 and Appendix C. For a given triplet (ν, η, ζ), we invert fundamentals as in Section 5.2. Next, we solve the steady-state and the FAME of our economy. We further simulate the dynamic response of the entire economy to a 1% transitory productivity shock, together with the corresponding amenity shock, localized in a randomly chosen location. We also simulate the dynamic response of the entire economy to a 1% capital depreciation shock localized in a randomly chosen location. From these counterfactual responses, we construct model analogs of the event study estimates from Section 4. We then use these model-based event study estimates to construct target moments that inform (ν, η, ζ).

Specifically, we denote by $\mathrm{irf}_{v,s,\theta}$ the model impulse response function corresponding to the event study estimates for outcome variable v, shock s, and parameters θ. The outcome v denotes either income per capita, population, or investment.[28] The shock s denotes either a joint productivity-amenity shock or a capital depreciation shock. We denote by $\mathrm{IRF}_{v,s}$ its counterpart in the data. We also denote by $\mathrm{cir}_{v,s,\theta}$ and $\mathrm{CIR}_{v,s}$ the model and data cumulative impulse responses. That is, for any impulse response irf and horizon h, we define $\mathrm{cir}_h = \sum_{h'=0}^{h} \mathrm{irf}_{h'}$.

We leverage a key property of the FAME to estimate the migration and investment elasticities without having to specify the magnitude of shocks. The response of the economy to shocks is linear in the magnitude of the shock by construction. Hence, relative impulse response are independent from the magnitude of a common shock. For instance, in the FAME, the impulse response of employment relative to the response of income per capita following a productivity shock is independent from the magnitude of this productivity shock. If we target relative impulse responses, we can thus use a shock of an arbitrary magnitude.

What moments are best fit for our purposes? Our strategy estimates the three parameters $\theta = (\nu, \zeta, \eta)$ jointly, but we discuss how we select each moment to provide intuition for identification. We provide numerical confirmation that these parameters determine the relevant moments below.

The gravity structure of migration indicates that the migration elasticity ν is related to the response of local population relative to the response of income per capita holding amenities fixed. If we could

---

[27]We use a Sobol sequence to cover the multivariate space more efficiently than with a standard tensor product grid.

[28]We use income per capita as the data counterpart of wages in the model to capture self-employment and business income that is not explicitly modeled. The model does not feature non-employment, so in principle we could use either employment or population in the data as a counterpart of population in the model. We use population in the data as it is the most natural counterpart of population in the model.

isolate a productivity shock in the data, we could use the response of population relative to income per capita. However, heat waves also cause amenity shocks, thereby leading to a well-known omitted variable problem. Thus, we use the response of population relative to investment, the latter being likely less directly sensitive to the response of amenities than income per capita.[29]

Specifically, we use the cumulative impulse response of local population relative to the cumulative impulse response of investment at 10 years after a productivity shock, $\frac{\text{cir}_{10,\text{pop,prod-am},\theta}}{\text{cir}_{10,\text{inv,prod-am},\theta}}$, to inform the migration elasticity ν. We target the corresponding moment in the data following a heat wave in warm counties. Intuitively, if population responds strongly relative to investment, the migration elasticity must be large.[30] We use cumulative impulse responses—or, equivalently, average impulse responses—rather than plain impulse responses because they are less sensitive to short-term, slow adjustment mechanisms that we do not model (e.g. sticky wages).

To inform the amenity-productivity ratio η, we use the cumulative impulse response of income per capita relative to the cumulative impulse response of local population at 10 years after a productivity shock, $\frac{\text{cir}_{10,\text{ipc,prod-am},\theta}}{\text{cir}_{10,\text{pop,prod-am},\theta}}$. We target the corresponding moment in the data following a heat wave in warm counties. Intuitively, if population responds strongly relative to income per capita holding the migration elasticity ν fixed, amenities must be a large component of the effect of heat waves.

The cumulative impulse response of population relative to investment 10 years after a capital depreciation shock, $\frac{\text{cir}_{10,\text{pop,cap dep},\theta}}{\text{cir}_{10,\text{inv,cap dep},\theta}}$ informs the investment elasticity ζ. Intuitively, the size of the population response encapsulates the overall magnitude of the shock. If investment responds strongly relative to population, the investment elasticity ζ must be large. We target its counterpart in the data following storms in coastal counties.
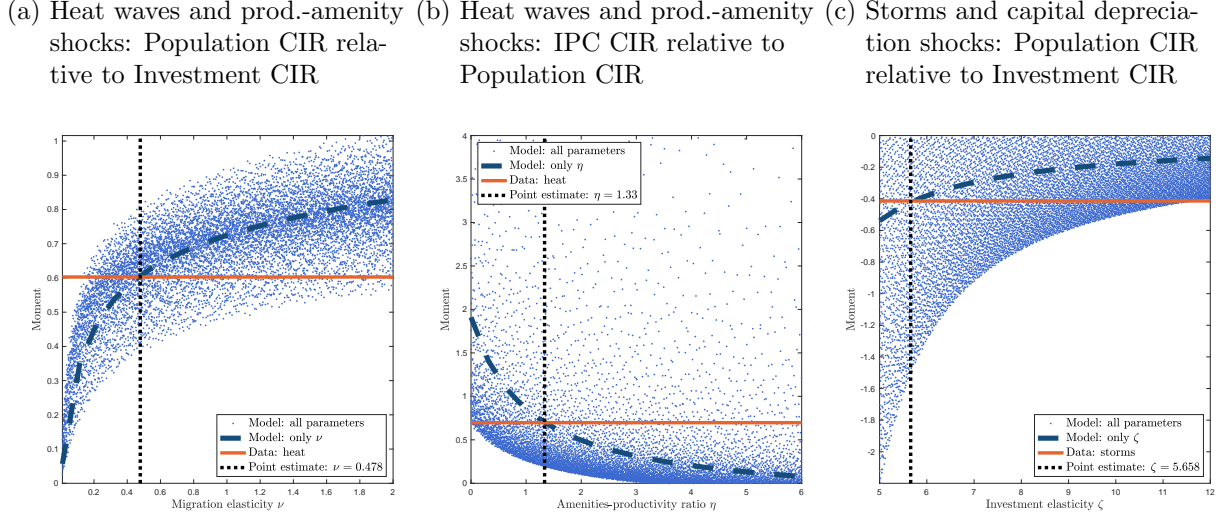
The computational speed of the FAME lets us handle the computational demands of our estimation strategy. We invert fundamentals, solve for the steady-state of the model, the FAME, and impulse responses for 10,000 triplets $\theta = (\nu, \eta, \zeta)$. We construct our target moments and contrast them with their data counterparts in Figure 6. The figure confirms our global identification argument numerically.

Panel 6(a) displays the cumulative response of population relative to investment following a productivity-amenity shock. Each blue dot is the relative cumulative response in the model, for a given triplet of parameter values (ν, η, ζ). We order results by the migration elasticity ν on the x-axis to highlight our identification argument in a multivariate and univariate sense. The impact of ν on the relative cumulative response on the y-axis manifests clearly in the upward-sloping relationship visible in the scatterplot: on average, across all possible values (η, ζ), a higher value of ν increases the response of population relative to investment (multivariate identification). The impact of the migration elasticity ν on the relative cumulative response is also visible in the upward-sloping relationship between the moment and the mi-

---

[29]Although we use indirect inference that explicitly accounts for the response of amenities to heat waves, we use a target moment that identifies the migration elasticity ν more sharply.

[30]In the model, population is related to the own migration share. Hence, our approach also resembles a gravity equation regression in which we instrument for the origin investment with heat waves.

Figure 6: Identification of migration and investment elasticities and amenity-productivity ratio.

(a) Heat waves and prod.-amenity shocks: Population CIR relative to Investment CIR

(b) Heat waves and prod.-amenity shocks: IPC CIR relative to Population CIR

(c) Storms and capital depreciation shocks: Population CIR relative to Investment CIR

Note: Blue dots: 10,000 model simulations sequencing parameter vectors $\theta = (\nu, \zeta, \eta)$ using a Sobol sequence in the cube $[0, 2] \times [5, 12] \times [0, 16]$. Dashed dark blue line: moment in the model when only the parameter on the x-axis varies, holding other parameters at their point estimate. Horizontal solid orange line: moment in the data. Vertical dashed black line: parameter estimate.

gration elasticity ν when we hold the other parameters (η, ζ) fixed at their point estimate (univariate identification).

Variation in the relative cumulative response on the y-axis conditional on ν along the x-axis captures how the investment elasticity ζ and the amenity-productivity ratio η also affect the relative cumulative response. Visually, the migration elasticity ν emerges as a key determinant of the cumulative response of population relative to investment following productivity-amenity shocks. Panel 6(a) also reports the relative cumulative response in the data for heat waves in warm counties.

Panel 6(b) depicts the cumulative response of income per capita relative to population following a productivity-amenity shock on the y-axis. The x-axis represents the productivity-amenity ratio η. This ratio emerges visually as a key determinant of the response of income per capita relative to population. We contrast the results from the model with the data following heat waves in warm counties.

Panel 6(c) depicts the cumulative response of population relative to investment following a capital depreciation shock on the y-axis. The x-axis represents the investment elasticity ζ. The investment elasticity emerges visually as a key determinant of the response of employment relative to investment. We contrast the results from the model with the data following storms in coastal counties.

We estimate the migration elasticity to be $\nu = 0.48$. Consistently with our county-level specification, our value is somewhat above the value of 0.2 in the state-level specification in Caliendo et al. (2019). We estimate that amenities respond $\eta = 1.33$ times more than productivity following heat waves. This relative response is four times larger than the average one in Cruz and Rossi-Hansberg (2023) for developed and developing countries. The larger relative role of amenities in the context of the U.S. is consistent with production being better shielded from extreme heat through adaptation such as air conditioning than in

developing nations. Our estimate of the investment elasticity $\zeta = 5.67$ implies adjustment costs that are somewhat less convex than quadratic, a common benchmark in the literature.

5.4 Damage functions

With the migration and investment elasticities in hand, we turn to estimating the damage functions for productivity, amenities, and capital depreciation. We do so in two steps. In the first step, we estimate economic damages from a given realization of storms and heat waves using the cumulative impulse responses from Section 4.4. In the second step, we interact these damages from single events with the change in the probability that these events occur as global mean temperatures rise, as shown in Figure 2.

In the first step of our estimation strategy, we estimate economic damages from a given realization of storms and heat waves by matching the magnitude of the cumulative impulse responses. As in Section 4, we leverage the linearity of the FAME. It implies that the size of the shock is equal to $\frac{\text{CIR}_{10,v,s}}{\text{cir}_{10,v,s,\hat{\theta}}}$, where $\text{cir}_{10,v,s,\hat{\theta}}$ denotes the cumulative impulse response of variable v to a 1% shock to s (productivity-amenity or capital depreciation) for the estimates of the triplet $\hat{\theta}$ we obtained above.

For heat waves in warm counties, we target the population response. Given that we match exactly the responses of population relative to investment and income per capita in Figure 6, we match exactly the cumulative response of population, investment, and income per capita 10 years out. We estimate storm damages in coastal counties by targeting the cumulative impact of storms on investment 10 years out. Given that we match exactly the population response relative to investment in Figure 6, we match exactly the cumulative investment response 10 years out.

In addition to matching exactly the cumulative response 10 years out, we ask whether the estimated model provides a plausible account of the time path of the impulse response function of targeted moments. Of course, our framework cannot be expected to match exactly the precise time path of income per capita, population, and investment responses jointly for each extreme event. Nevertheless, Figure 7 displays impulse responses in the model and in the data for heat waves in warm counties.

Figure 7 displays the investment, population, and income per capita impulse responses in the data (circles and dotted line) and in the model (solid line) following heat waves in warm counties. Because we match the 10-year cumulative response, the areas under the impulse response in the model and in the data match exactly. Figure 7 reveals that the model provides a reasonable account of the full time path of the response of investment population and wages to heat waves. For all three outcomes, the response in the model lies within the 95% confidence interval around the empirical point estimates for nearly all horizons.

Our impulse response-matching exercise implies that a 1-in-20-years heat wave causes a $D_{\text{warm}}^{\text{heat,prod.}} \equiv$ 5.1% negative productivity shock to a warm county, accompanied by a $D_{\text{warm}}^{\text{heat,am.}} \equiv 6.8\%$ reduction in local amenities. This impact is sizeable. Yet, it is lower than the local effects estimated for locations in

Figure 7: Heat waves: impulse responses in model and in data.

(a) Investment (b) Population (c) Income per capita
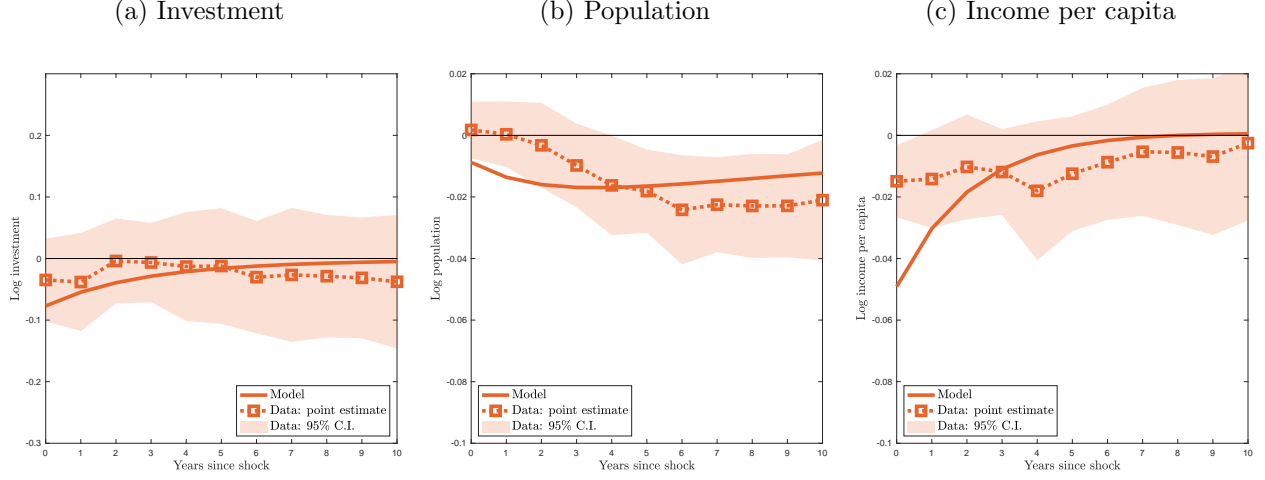
Note: Impulse responses for investment (a), population (b), and income per capita (c) after a 1-in-20-years heat wave in a warm county. For (c) we use the response of wages, w_{it}, in the model and income per capita in the data.

the entire world, including developing countries. For instance, Cruz and Rossi-Hansberg (2023) find that the productivity effect in the warmest locations across the world can exceed 15%.

Figure 8 displays the investment, population, and income per capita impulse responses in the data (circles and dotted line) and in the model (solid line) following storms in coastal counties. Figure 7 reveals that the model provides a reasonable account of the full time path of the response of investment and population to storms. The untargeted response of income per capita is flatter in the data than in the model. However, for all three outcomes, the response in the model lies within the 95% confidence interval around the empirical point estimates for nearly all horizons.

Our impulse response-matching exercise implies that a 1-in-50-years storm causes a $D_{\text{coastal}}^{\text{storm}} \equiv 17\%$ negative capital depreciation shock to a coastal county. This impact is substantial and, to the best of our knowledge, is a new estimate to the literature.

We now turn to the second step of our estimation strategy. To construct damage functions that depend on global mean temperatures, we interact our estimates of shocks ($D_{\text{coastal}}^{\text{storm}}, D_{\text{warm}}^{\text{heat,prod.}}, D_{\text{warm}}^{\text{heat,am.}}$) with secular changes in the probability of the corresponding events. These changes are similar to those in Figure 2, but we construct trends location by location. To estimate secular changes in the probability of extreme events for each location, we simply regress the change in the probability of an event $e \in \{\text{storm}, \text{heat}\}$, p_{it}^e, for each location i on changes in global mean temperatures T_t:

$$\Delta p_{it}^e = \text{cst} + p_{i1}^e \Delta T_t + \varepsilon_{it}.$$

Figure 8: Storms: impulse responses model and in data.

(a) Investment   (b) Population   (c) Income per capita
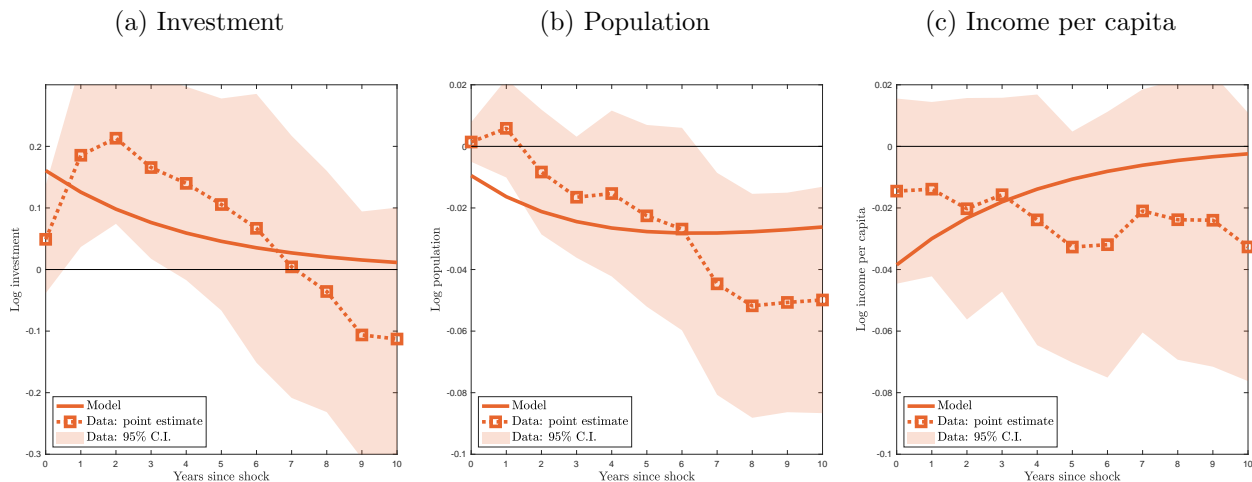
Note: Impulse responses for investment (a), population (b), and income per capita (c) after a 1-in-50-years storm in a coastal county. For (c) we use the response of wages, w_{it}, in the model and income per capita in the data. The 10-year cumulative impulse response for investment (a) and population (b) are targeted. The impulse response for income per capita is untargeted.

Finally, we construct damage functions according to

$$\delta_{i1} = \mathbb{1}\{i \text{ is coastal}\}p_{i1}^{\text{storm}}D_{\text{coastal}}^{\text{storm}}, \quad \chi_{i1} = \mathbb{1}\{i \text{ is warm}\}p_{i1}^{\text{heat}}\frac{D_{\text{warm}}^{\text{heat,prod.}}}{\psi_{\text{warm}}^{\text{heat}}}, \quad a_{i1} = \mathbb{1}\{i \text{ is warm}\}p_{i1}^{\text{heat}}\frac{D_{\text{warm}}^{\text{heat,am.}}}{\psi_{\text{warm}}^{\text{heat}}},$$

where $\psi_{\text{warm}}^{\text{heat}}$ denotes the estimated mean-reversion coefficient of productivity following heat-waves.[31] To have sufficient statistical precision in practice, we construct 100 clusters of contiguous counties based on coastal status and annual mean temperature, and estimate the slopes p_{i1}^{e} at the cluster level.

Figure 9 maps our estimated damage functions. Panel 9(a) shows the impact of a 1°C increase in global mean temperatures on productivity for every county in the U.S. The impact is highly heterogeneous across space. We find that southern Florida will experience productivity reductions of 5% due to the rapidly rising occurrence of heat waves. For a 3°C warming scenario, this reduction compounds to a 15% reduction in productivity. Productivity losses of comparable magnitude are pervasive throughout the South of the U.S. Northern Texas and Oklahoma gain moderately, as our historical data shows that they experienced a reduction in the frequency of heat waves. By construction, the change in amenities is proportional to the change in productivity and thus we omit the corresponding map.

Panel 9(b) shows the impact of a 1°C increase in global mean temperatures on capital depreciation for every county in the U.S. The impact is highly heterogeneous across space and only imperfectly correlated with the one for heat waves. Storms increase capital depreciation rates substantially in the South-Eastern Atlantic coast. In Louisiana and North and South Carolina, a 1°C increase in global temperature increases the capital depreciation rate by 4 p.p. This effect amounts to a 12 p.p. increase for a warming scenario of 3°C, more than doubling the baseline capital depreciation rate. These capital depreciation effects are

---

[31]We estimate $\psi_{\text{warm}}^{\text{heat}}$ by targeting the shape of the impulse response for income per capita.

Figure 9: Damage functions from heat and storms in the United States.

(a) Change in log productivity

(b) Change in annual capital depreciation
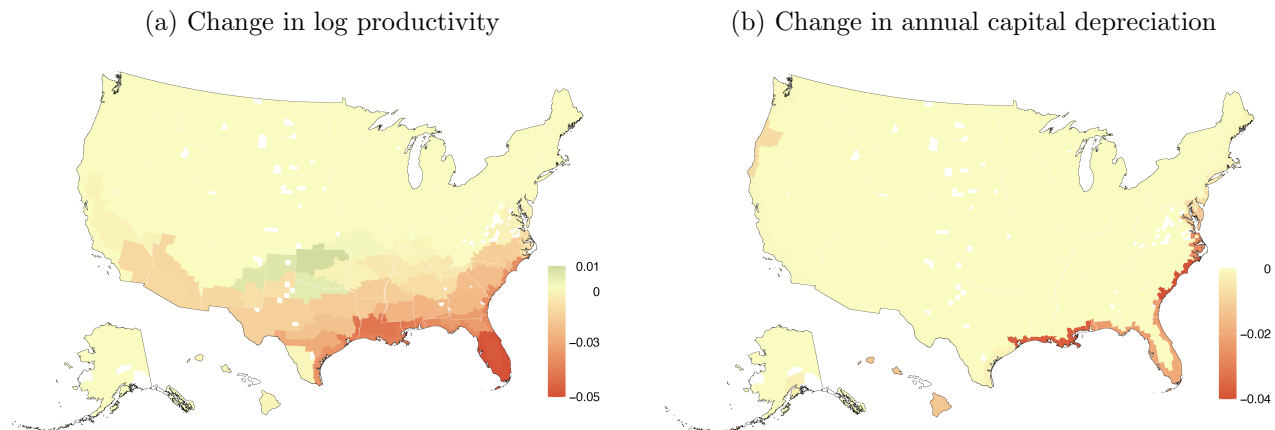
Note: The effect of a 1°C increase in global temperature on productivity and annual capital depreciation rates across counties in the U.S. Panel (a): coefficients χ_{i1} such that $d \log Z_{it} = \chi_{i1} dT_t$. Panel (b): negative of coefficients δ_{i1} such that $d\delta_{it} = \delta_{i1} dT_t$.

substantial, but affect a much smaller fraction of counties than heat waves. Through the lens of our structural model, we can compare their relative importance.

6   The impact of climate change

With our estimated damage functions at hand, we evaluate the impact of climate change on welfare and allocations. We start the economy in steady-state. We use 2023 as the year in which individuals learn the path of warming T_t^D and start reacting to it. We use a warming scenario T_t^D that increases temperatures by 3°C in 2100 relative to 2023, and by 4°C by 2300. This temperature path is consistent with the business-as-usual scenario put forward by the IPCC and the current slope of warming reported in Figure 1.[32] Because the impact of shocks is linear in the FAME, the effect of another scenario with a different final temperature can be obtained by rescaling our results. For example, we can scale changes down to account for possible mitigation efforts within the century, as captured by other IPCC scenarios.

6.1   Aggregate damages from climate change

We uncover substantial effects of climate change on welfare. Table 1 reports the impact of climate change on workers and capitalists in 2023 and 2100. In 2023, workers already lose 4.9% in consumption-equivalent welfare on average. This substantial impact represents an annual loss of consumption of \$3,005 to the average resident of the U.S.[33] For comparison, estimates from the gains from trade for the U.S.—i.e. the benefits from moving from autarky to current trade—are typically less than 3%.[34]

---

[32]Given the warming of 1°C in 2023 relative to pre-industrial temperatures, this warming scenario corresponds to 4°C warming relative to pre-industrial temperatures by 2100.

[33]The Bureau of Labor Statistics reports average annual expenditures of \$61,334 in 2020.

[34]See for example Costinot and Rodríguez-Clare (2014).

Table 1: Impact of climate change on welfare and allocations.

	Welfare				Allocations	
	Workers		Capitalists		Population	Capital
	2023	2100	2023	2100	2100	2100
Baseline						
Aggregate (%)	-4.9	-11.6	-0.8	-13.4		-31.8
St.dev. (p.p.)	2.4	4.2	5.6	46.4	40.8	45.9
Discount rate: Aggregate (%)						
5%	-3.4	-12.0	-0.5	-12.8		-32.0
2%	-6.2	-12.0	-0.6	-12.2		-33.8
1%	-8.5	-12.4	-0.6	-11.9		-34.7
By type of damages: Aggregate (%)						
Capital depreciation	-2.2	-5.3	-0.7	-11.6		-23.9
Temperature	-2.7	-6.3	-0.1	-1.8		-7.9
Productivity	-1.3	-3.1	-0.1	-2.3		-5.8
Amenities	-1.4	-3.2	0.0	0.5		-2.2
No climate anticipations: Workers and capitalists						
Aggregate (%)	-4.8	-11.5	-0.5	-13.1		-29.5
St.dev. (p.p.)	2.4	4.7	3.9	43.1	36.9	42.4
No adaptation: Fixed population						
Aggregate (%)	-4.8	-11.3	-0.6	-12.6		-20.1
St.dev. (p.p.)	8.7	16.3	1.8	22.8	0	24.1

Crucially, these losses arise because of anticipations of future climate change. In our evaluation in 2023, climate change is just starting. Workers anticipate that climate conditions will worsen in the future, lowering productivity and amenities, depreciating capital, and ultimately affecting future real wages and the present value of future consumption streams, which are discounted at 3% annually. By 2100, once climate change has mostly materialized, welfare losses to workers are much larger—11.6% in consumption equivalent terms—because most climate damages are no longer discounted. This impact amounts to an annual loss equivalent to \$7,115 out of current consumption expenditures.[35]

Capitalists are initially less exposed to climate change. In 2023, their welfare loss is only 0.8%. However, their exposure grows faster over time. By 2100, the welfare losses to capitalists reach 13.4% in the aggregate. This sizable effect is largely driven by a dramatic 31.8% reduction in the aggregate capital stock of the U.S. because of climate change. The welfare loss to capitalists is only half of the reduction in the aggregate capital stock because of general equilibrium effects: as capital becomes scarcer, its return

---

[35]Our framework does not feature permanent economic growth. Yet, assuming a 3% annual growth rate, our results imply that in 2100 climate change represents a \$69,283 annual consumption loss for the average resident of the U.S.

rises, which offsets part of the losses to capitalists.

6.2 The spatial distribution of climate damages

How unequally distributed are the welfare losses from climate change? Figure 10 depicts the spatial distribution of the impact of climate change on welfare and allocations. Panel 10(a) displays 2023 welfare losses to workers in each county relative to the aggregate. Counties in green are counties that are better off than the average county—although this does not imply that these counties gain from climate change. Counties in orange are counties that are worse off than the average county.

We find that workers in almost all counties lose from climate change in 2023. Workers in the South-East of the U.S. are particularly exposed. The combination of more frequent heat waves and destructive storms on the coast implies that residents of multiple counties in Louisiana lose more than 15% ($9,200 annually) because of climate change in 2023. Losses above 10% in 2023 ($6,133 annually) are experienced in Texas, Florida, and North and South Carolina. By 2100, the spatial distribution of welfare losses from climate change is highly correlated with the spatial distribution in 2023, as evidenced by panel 10(c). The magnitude of losses, however, is much larger. Residents of coastal counties in Louisiana are more than 30% worse off in 2100 because of climate change.

Capitalists experience much more unequal impacts from climate change, as shown in panel 10(b). Owners of capital in southern coastal Louisiana, Georgia, and North and South Carolina experience welfare losses in excess of 20% in consumption-equivalent welfare in 2023 because of climate change. This concentration of large damages in coastal areas and negligible impacts in inland counties implies that the standard deviation of welfare losses for capitalists in 2023 (5.6 p.p.) is more than twice the standard deviation of welfare losses for workers (2.4 p.p.), as shown in Table 1.

Welfare losses to capitalists are more unequally distributed than those for workers because capital cannot move, while workers can. Migration provides an important adaptation strategy that spreads losses from climate change more equally across workers. Owners of an immobile capital stock do not have that option. As a group, capitalists can only let the capital stock depreciate in locations that experience adverse climate change, and invest anew in the places where comparative advantage rises.

By 2100, inequality among capitalists skyrockets (see panel 10(d)). Owners of capital on the South-Eastern coast of the U.S. lose in excess of 50% in consumption-equivalent welfare. Over 77 years, however, workers have time to migrate to less affected areas, increasing the return to capital there. Thus, capitalists in the North of the U.S. experience substantial gains that can exceed 50% in consumption equivalent terms.

We find that migration responds substantially to climate change. Panel 10(e) reveals that counties that are heavily exposed to extreme heat and storms in the South-East lose more than half of their population by 2100. While coastal counties in Florida lose most of their population, the state as a whole loses 46% of its residents. These workers move to Northern counties that are shielded from these adverse effects, some of which double their population. These population movements reflect the changing comparative

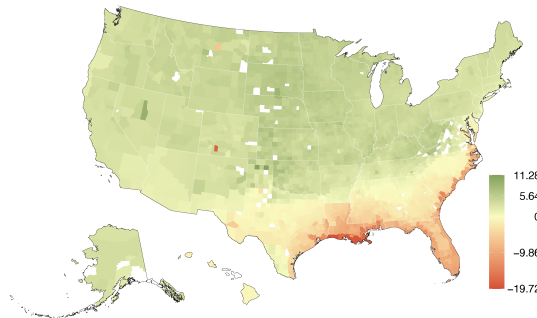Figure 10: Impact of 3°C additional warming by 2100

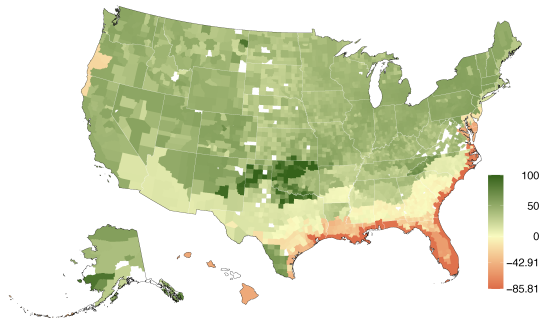(a) Worker welfare in 2023
Relative to aggregate (-4.9%)
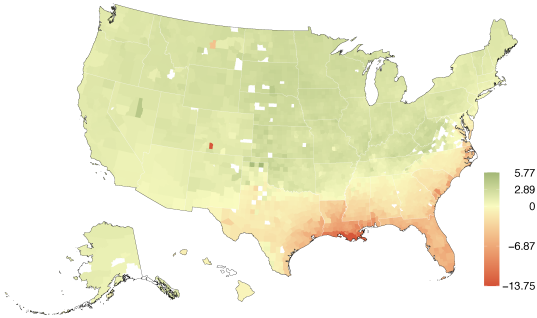
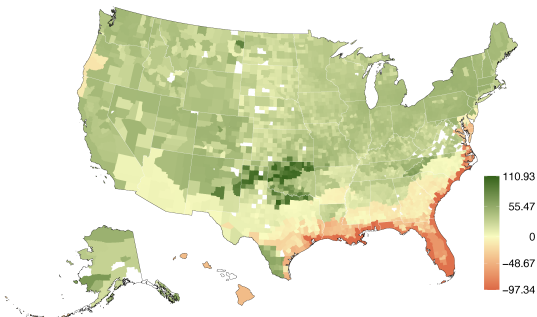(b) Capitalist welfare in 2023,
Relative to aggregate (-0.8%)
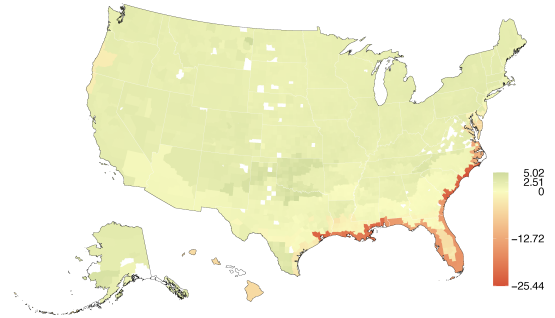
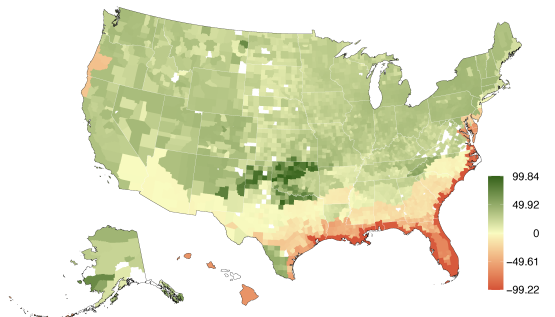(c) Worker welfare in 2100,
Relative to aggregate (-11.6%)

(d) Capital owner welfare in 2100,
Relative to aggregate (-13.4%)

(e) Population change in 2100

(f) Capital stock change in 2100

advantage of locations. As workers reallocate, the rental rate of capital adjusts accordingly, imposing additional losses to capitalists in locations that lose population. Over time, changes in the local stock of capital are highly correlated with population movements as shown in panel 10(f). Capital is no longer profitable once workers have left, and capitalists in Northern locations invest heavily to accommodate higher demand for capital and housing.

Our results highlight that climate damages—and the ensuing reallocation of economic activity—are substantial. Critically, we find large economic damages because we constrain the model to match our empirical event study results using a relatively large discount rate of 3%. In the 'Discount rate' section of Table 1, we analyze how discounting affects climate damages. Consistent with the climate change literature,[36] we find that lower discount rates increase welfare losses from climate change for workers in 2023 since climate damages remain back-loaded then. By 2100, climate change has mostly already occurred in the simulation and the discount rate does not affect worker welfare that much anymore. The patterns are reversed for capitalists. This reversal takes place because of two offsetting forces. Similarly to workers, when the discount rate falls, capitalists value back-loaded damages more. However, when the discount rate falls, the cost of funding goes down because the interest rate goes down, which makes reallocating capital and investing cheaper. In 2023, these two effects offset each other. In 2100, the 'damage valuation effect' largely vanishes because climate change has mostly already happened, leaving only the 'cost of funding effect' operative. As a result, in 2100, the lower the discount rate, the lower the losses to capitalists.

Having established the magnitude of climate damages, we now study the role of anticipation and adaptation using three distinct counterfactual exercises.

6.3   Capital depreciation and temperature

Our first exercise highlights the role of anticipation in forward-looking capital investment decisions. Introducing anticipation through the FAME lets us study the role of climate change on capital depreciation. How large is this novel role of anticipation and capital depreciation relative to the role of heat waves? The linearity of the FAME lets us propose an exact additive decomposition.

Table 1 reveals that the impact of capital depreciation is substantial. Despite affecting only a small subset of locations, repeated capital destruction due to rising storm activity in coastal counties accounts for 88% of aggregate welfare losses to capitalists and for 45% of aggregate welfare losses to workers in 2023. Temperature accounts for the remaining 12% and 55%, respectively.

The capital depreciation channel also accounts for 75% of the reduction of the capital stock due to climate change in the U.S. This effect reflects both the direct depreciation effect as well as reduced incentives to invest in counties that have high capital depreciation rates. Temperature is responsible for the remaining 25% of the reduction in the capital stock. As productivity drops because of extreme heat,

---

[36]See, for example, Heal (2017) for a discussion of discount rates in the climate change literature.

capital becomes less valuable and investment falls. The effects of heat waves can be further split into productivity and amenity effects. Table 1 indicates that they contribute nearly equally to the welfare losses of workers in 2023 and 2100.[37]

6.4 Anticipation

In a second exercise, we shut down climate change anticipation by either workers or capitalists. In this counterfactual, workers or capitalists experience the effect of the current and past changes in temperatures but they believe that future temperatures will remain as in the current period. Hence, their actions incorporate no anticipation effects.

We find that anticipation leads to substantial mobility. When individuals fail to anticipate future climate change, mobility falls. Figure 11(a) reveals that the gap with the baseline scenario is largest close to 2050. By 2050, the standard deviation of population changes is 7 p.p. lower when both workers and capitalists do not anticipate climate change, and 4 p.p. lower when only workers do not. These impacts represent a substantial fraction—32% and 18%, respectively—of the baseline gross mobility rate. Of course, the decline in mobility due to lack of anticipation is a transitory phenomenon: in the long run, anticipations do not affect decisions anymore once the economy converges back to a new steady-state.

Anticipation increases mobility because climate change builds up slowly over time. Individuals who anticipate future climate internalize that their location will become worse than it is today. As a result, they move out more rapidly. Crucially, the anticipation of workers and capitalists reinforce each other: when capitalists do not anticipate future climate change, they keep investing in locations that will deteriorate in the future. This excess investment further keeps workers in place through a larger capital stock, higher nominal wages, and lower housing prices.[38]

Since the future climate is correlated with the current climate, the locations in which anticipation lead to the largest mobility gaps are also those where climate change has the largest effect in the baseline warming scenario. Panel 11(e) highlights that the South-East of the U.S. loses less population when workers and capitalists fail to anticipate future climate. In Louisiana, Florida, and coastal counties in North and South Carolina, these effects are large and can offset as much as half of the baseline decline in 2050.

Without anticipation, welfare is more unequally distributed than with anticipation. Individuals in locations that suffer most from climate change experience larger losses without anticipation because they

---

[37]When we include the effects of extreme cold in the analysis using the event study results in Appendix D.3, we find that the reduction in extreme cold delivers moderate 0.7% gains for workers in the U.S. If we factor in cold waves into our analysis, damages to the capital stock then account for over half of the welfare losses of workers, which amount to 4.2% in this case.

[38]In Figure 17, Appendix F, we also consider an alternative scenario in which individuals learn of future climate change several years before global temperatures start rising in 2023. In this case, individuals take anticipatory actions, and population and capital stocks in 2023 already differ from steady-state. If individuals learn of climate change at least by 2000, the standard deviation of population changes in 2023 is above 9 p.p.

Figure 11: The impact of shutting down anticipations on mobility and welfare.
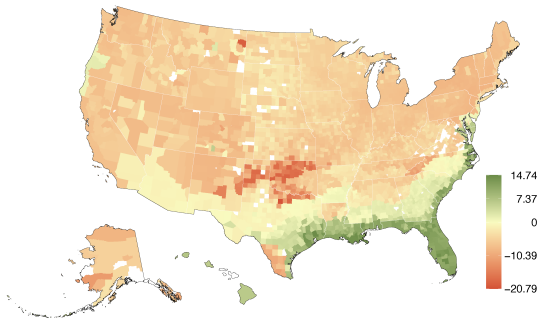
(a) Population change dispersion relative to baseline.
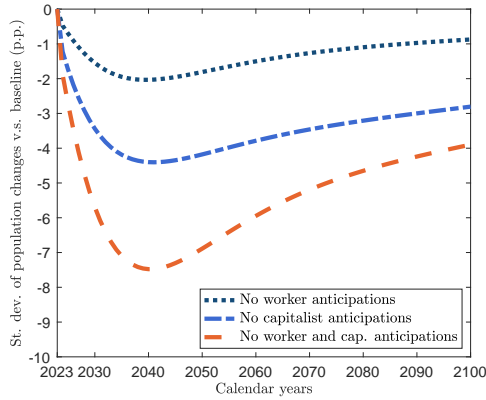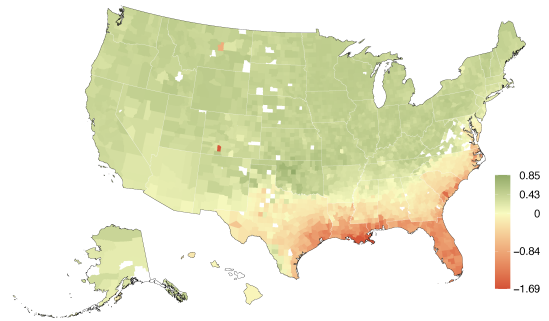

(b) Capital change dispersion relative to baseline.
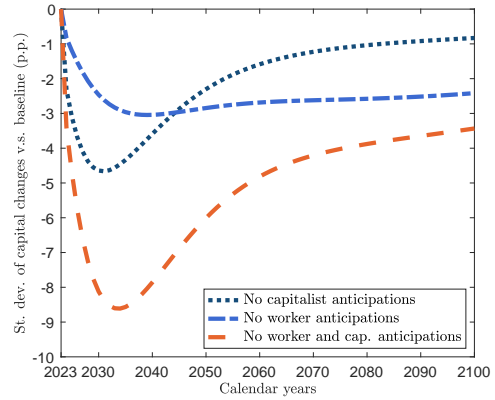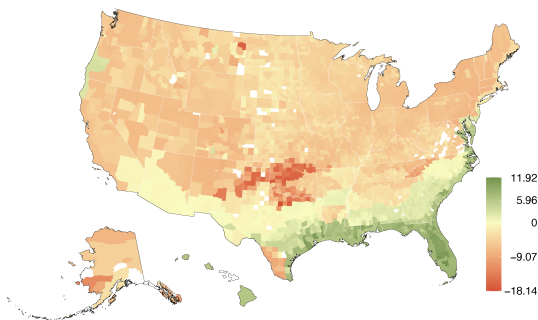

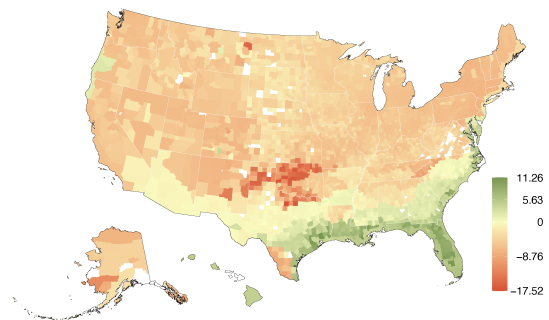(c) Relative population change in 2050 (p.p.).

(d) Relative worker welfare change in 2050 (p.p.).

(e) Relative capital change in 2050 (p.p.).

(f) Relative capitalist welfare change in 2050 (p.p.).

fail to pre-emptively out-migrate or divest and are continuously surprised by a worsening climate. Panel 11(f) shows that workers in Florida who do not anticipate climate lose an additional 0.65% of welfare ($397 per year) by 2050. Across the U.S., the standard deviation of welfare is 0.5 p.p. higher without anticipations, 13% above the baseline warming scenario. However, despite this higher dispersion, aggregate welfare of workers and capitalists are largely unchanged by the lack of anticipation. The additional losses in exposed locations are offset by relative gains in non-exposed counties. We summarize these results in the 'No Anticipation' section of Table 1 when both workers and capitalists do not anticipate climate change.[39]

6.5 Adaptation

The third exercise highlights the role of adaptation through migration. We evaluate the impact of global warming when we shut down migration completely, i.e. $\mu = 0$ in the 'Adaptation' section of Table 1.[40] Welfare losses for workers are much more spatially concentrated absent migration. Figure 12(a) reveals that workers in coastal counties in the South-East lose an additional 20% in welfare terms in 2023 when they cannot move. Welfare losses in these areas in 2023 can thus exceed 25% ($15,334 per year) without migration. Across the U.S., the standard deviation of welfare losses of workers rises to 8.7 p.p. from 2.4 p.p. in 2023.

Capitalists benefit when workers remain in place. Abundant labor raises the return to capital. Panel 12(b) shows that relative capitalists gains in 2023 are the mirror image of worker losses. Overall, the dispersion of capitalist welfare losses drops from 5.6 p.p. in the baseline to 1.8 p.p. when migration is shut down.

Perhaps surprisingly, migration has a negligible effect on aggregate welfare losses for workers, despite its sizeable effect on welfare dispersion. Our welfare decomposition in Proposition 5 and in equation (18) sheds light on this result. The primary channel through which migration affects welfare is through the option value to migrate once the comparative advantage of locations changes. This effect is large in the cross-section. Yet, equation (18) shows that the option value drops out exactly in the aggregate.

The welfare decomposition in Proposition 5 and in equation (18) indicate that migration may operate through additional reallocation channels. We find these channels to be quantitatively small in the U.S. with current climate damage functions. Figure 12(c) displays the welfare decomposition from Proposition 5 in our baseline calibration.

In 2023, there is no role for any reallocation component, because by definition reallocation only happens gradually over time. Thus, in 2023, the direct impact of climate change constitutes 100% of climate damages. We find that the irrelevance result from equation (18) holds quantitatively: the option

---

[39]Table 2 in Appendix F presents results for the cases where either workers or capitalists do not anticipate climate change.
[40]We do not consider a counterfactual with fixed capital because we would have to assume away damages to the capital stock, which are important both quantitatively and in determining the geography of losses from climate change.

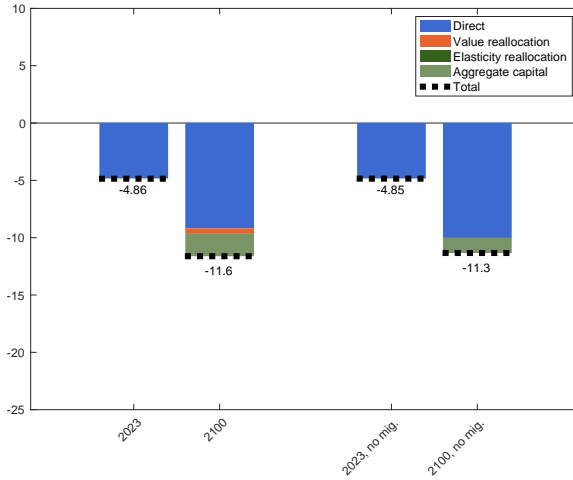Figure 12: The impact of shutting down migration.

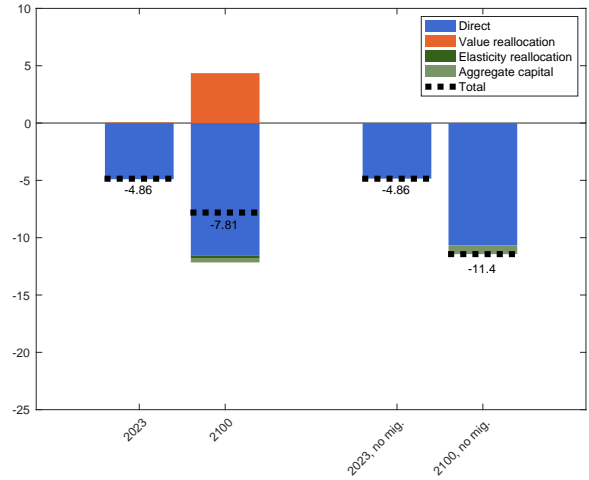(a) Relative worker welfare change in 2023 (p.p.).
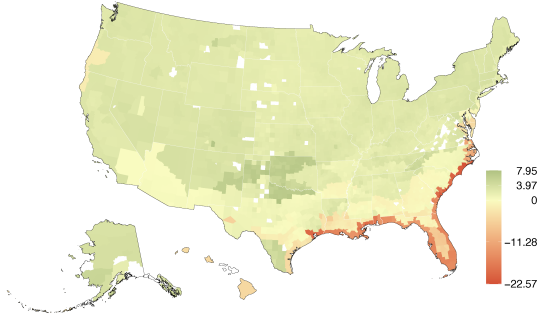
(b) Relative capitalist welfare change in 2023 (p.p.).
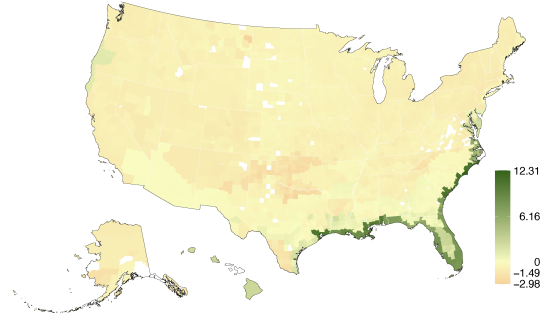
(c) Welfare decomposition in baseline scenario.

(d) Welfare decomposition with correlated damages.

Note: Welfare decomposition from Proposition 5 in baseline model (a) and in model with correlated damages (b). Correlated damages defined as $\tilde{x}_{i1} = \bar{x}(\max_j V_j^{SS} - V_i^{SS})^4$ for $x \in \{\chi, a, \delta\}$ and where $\bar{x}$ is chosen so that the relative importance of temperature and capital depreciation, as well as aggregate damages, are identical to the baseline model.

value of migration does not affect welfare losses, which remain near 4.9% with and without migration. By 2100, the value reallocation channel becomes active but is negative and small. The aggregate capital depreciation channel imposes additional losses because the aggregate capital stock is lower primarily due to storms.[41]

Crucially, the irrelevance of migration as an aggregate adaptation mechanism is a feature of U.S. data, not of migration in general. In the U.S., climate damages—and hence migration patterns—are largely

---

[41]Perhaps surprisingly, shutting down migration delivers slight gains—0.2% out of 11.6%—given our utilitarian social welfare function in Appendix B.6. This result arises because our utilitarian social welfare function weights individuals by their location rather than by their type, which is defined by their location as well as their idiosyncratic preference. Hence, the Pareto frontier changes when comparing the economy with and without migration (Fajgelbaum and Gaubert, 2020). Consistently, we find that migration can deliver small gains (less than 1%) when we lower the number of locations or increase the migration elasticity, implying that preference shocks are less dispersed. In any case, these forces are small compared to the overall impact of climate change. Defining the appropriate welfare function accounting for dynamic migration with infrequent draws of preference shocks is beyond the scope of this paper and thus left for future work.

uncorrelated with the initial valuations of locations. As a result, the value reallocation component does not contribute significantly to welfare.

In principle, however, the value reallocation channel could be large. As an example, we construct an economy in which climate damages are perfectly negatively correlated with baseline valuations of locations and are highly spatially concentrated. In this economy, climate change pushes workers out of low-valuation locations and into high-valuation locations, thereby generating a high value of reallocation. Figure 12(d) displays the welfare decomposition in this artificial economy, where we calibrate the overall magnitude of damages to match the magnitude in our baseline economy and only change their spatial distribution.

When climate damages are negatively correlated with baseline location valuations and highly concentrated, migration becomes a powerful adaptation mechanism in the aggregate and offsets a large fraction of welfare losses. In our artificial economy, migration offsets as much as 32% of welfare losses by 2100, largely due to value reallocation. Thus, we emphasize that the irrelevance of migration as an aggregate adaptation mechanism may not hold in other environments.[42]

7 Conclusion

We have proposed a quantitative dynamic spatial assessment model of the U.S. economy. The model features forward-looking migration and capital investment decisions and can be quantified at the county level, namely, for the 3,143 counties in the U.S. economy. Importantly, because of the methodological advances we employ to solve for the dynamic equilibrium of the model, a numerical solution can be computed in a matter of seconds. We leverage this feature to structurally estimate the migration and investment elasticities, two key parameters that determine adaptation responses in the model. To quantify the damage functions that map global temperature increases with increases in local capital depreciation rates, amenities, and productivity, we use an extensive dataset of daily precipitation, windspeed, and temperatures since 1900 at the county level. This data, together with economic information at the county level, allowed us to estimate reduced-form reaction functions on several economic outcomes. We choose migration and investment elasticities, as well as damage functions, that make the model match this reduced form evidence. The resulting quantified model yields damages from a 3°C increase in average world surface temperatures that are about twice as large as what alternative models without an effect on capital depreciation yield for the U.S. (e.g. Cruz and Rossi-Hansberg, 2023).

Using this framework we reach three distinct conclusions. First, accounting for the effect of temperature on capital depreciation, through the impact of more frequent storms, is essential to obtain more

---

[42]For instance, at the world level one may hypothesize that exposure to climate damages is negatively correlated with valuations of locations, as low-income countries are more exposed to climate change. The value reallocation channel would then be large and positive. In that case, migration would mitigate the welfare effects of climate in the aggregate, as in Cruz and Rossi-Hansberg (2023).

accurate estimates of the welfare losses of climate change. Second, anticipation has small average effects on welfare but leads to large increases in migration flows, and large changes in the geography of investment, as workers and capitalists correctly anticipate the persistence of climate damages in particular regions. Finally, in the U.S., migration also has a very small average impact on welfare, but it leads to substantial increases in the dispersion of worker and capitalist welfare across locations; worker movements increase the losses in the value of capital at locations harmed by climate change.

Inevitably, our analysis abstracts from a number of potentially important mechanisms. One of them is costly trade in goods and heterogeneous climate effects by sector. Another is the differential effect temperature increases can have on people with heterogeneous skills, incomes, or assets. Finally, it is essential to incorporate risk and account for the uncertainty in climate predictions. To do so, we need to rely on second rather than first-order approximations of the "Master Equation". This methodology has also been developed by Bilal (2021) and we plan to use it to study the importance and implications of climate risk in subsequent work.

References

Bakkensen, Laura and Barrage, Lint (2018). "Climate Shocks, Cyclones, and Economic Growth: Bridging the Micro-Macro Gap". *National Bureau of Economic Research Working Paper 24893.*

Balboni, Clare (2021). "In Harm's Way? Infrastructure Investments and the Persistence of Coastal Cities". *Working Paper.*

Bilal, Adrien (2021). "Solving Heterogeneous Agent Models with the Master Equation". *Working Paper.*

Caliendo, Lorenzo, Dvorkin, Maximiliano, and Parro, Fernando (2019). "Trade and Labor Market Dynamics: General Equilibrium Analysis of the China Trade Shock". *Econometrica* 87.3, pp. 741–835.

Cardaliaguet, Pierre, Delarue, Francois, Lasry, Jean-Michel, and Lions, Pierre-Louis (2019). *The Master Equation and the Convergence Problem in Mean Field Games.* ISBN: 9780691190709.

Conte, Bruno, Desmet, Klaus, and Rossi-Hansberg, Esteban (2022). *On the Geographic Implications of Carbon Taxes.* Working Paper 30678. National Bureau of Economic Research.

Costinot, Arnaud and Rodríguez-Clare, Andrés (2014). "Chapter 4 - Trade Theory with Numbers: Quantifying the Consequences of Globalization". In: *Handbook of International Economics.* Ed. by Gita Gopinath, Elhanan Helpman, and Kenneth Rogoff. Vol. 4. Handbook of International Economics. Elsevier, pp. 197–261.

Courtier, P., Thépaut, J.-N., and Hollingsworth, A. (July 1994). "A Strategy for Operational Implementation of 4D-Var, Using an Incremental Approach". *Quarterly Journal of the Royal Meteorological Society* 120.519, pp. 1367–1387.

Cram, et al. (July 2015). "The International Surface Pressure Databank Version 2". *Geoscience Data Journal* 2.1, pp. 31–46.

Cruz, José-Luis and Rossi-Hansberg, Esteban (2023). "The Economic Geography of Global Warming". *Review of Economic Studies*, forthcoming.

Cruz, José-Luis (2021). "Global Warming and Labor Market Reallocation". *Working Paper.*

Cucchi, et al. (Sept. 8, 2020). "WFDE5: Bias-Adjusted ERA5 Reanalysis Data for Impact Studies". *Earth System Science Data* 12.3, pp. 2097–2120.

Dell, Melissa, Jones, Benjamin F., and Olken, Benjamin A. (2012). "Temperature Shocks and Economic Growth: Evidence from the Last Half Century". *American Economic Journal: Macroeconomics* 4.3, pp. 66–95.

— (2014). "What Do We Learn from the Weather? The New Climate–Economy Literature". *Journal of Economic Literature* 52.3, pp. 740–798.

Deryugina, Tatyana (2013). "The Role of Transfer Payments in Mitigating Shocks: Evidence from the Impact of Hurricanes". *SSRN Working Paper.*

Deryugina, Tatyana and Hsiang, Solomon (2017). "The Marginal Product of Climate". *National Bureau of Economic Research Working Paper 24072.*

Deschênes, Olivier and Greenstone, Michael (2011). "Climate Change, Mortality, and Adaptation: Evidence from Annual Fluctuations in Weather in the US". *American Economic Journal: Applied Economics* 3.4, pp. 152–85.

Desmet, Klaus, Kopp, Robert E., Kulp, Scott A., Nagy, Dávid Krisztián, Oppenheimer, Michael, Rossi-Hansberg, Esteban, and Strauss, Benjamin H. (2021). "Evaluating the Economic Cost of Coastal Flooding". *American Economic Journal: Macroeconomics* 13.2, pp. 444–86.

Desmet, Klaus, Nagy, Dávid Krisztián, and Rossi-Hansberg, Esteban (2018). "The Geography of Development". *Journal of Political Economy* 126.3, pp. 903–983.

Desmet, Klaus and Rossi-Hansberg, Esteban (2015). "On the Spatial Economic Impact of Global Warming". *Journal of Urban Economics* 88, pp. 16 –37.

Fajgelbaum, Pablo D. and Gaubert, Cecile (2020). "Optimal Spatial Policies, Geography, and Sorting". *The Quarterly Journal of Economics* 135.2, pp. 959–1036.

Fried, Stephie (Dec. 2021). "Seawalls and Stilts: A Quantitative Macro Study of Climate Adaptation". *The Review of Economic Studies* 89.6, pp. 3303–3344.

Harris, et al. (Mar. 15, 2014). "Updated High-Resolution Grids of Monthly Climatic Observations - the CRU TS3.10 Dataset: Updated High-Resolution Grids of Monthly Climatic Observations". *International Journal of Climatology* 34.3, pp. 623–642.

— (Apr. 3, 2020). "Version 4 of the CRU TS Monthly High-Resolution Gridded Multivariate Climate Dataset". *Scientific Data* 7.1, p. 109.

Heal, Geoffrey (2017). "The Economics of the Climate". *Journal of Economic Literature* 55.3, pp. 1046–63.

Hersbach, et al. (July 2020). "The ERA5 Global Reanalysis". *Quarterly Journal of the Royal Meteorological Society* 146.730, pp. 1999–2049.

Hsiang, Solomon M and Jina, Amir S (2014). "The Causal Effect of Environmental Catastrophe on Long-Run Economic Growth: Evidence From 6,700 Cyclones". *National Bureau of Economic Research Working Paper 20352*.

IPCC (2022). "Climate Change 2022: Impacts, Adaptation and Vulnerability". *Cambridge University Press*, pp. 37–118.

Kim, Hyungjun (June 1, 2017). *Global Soil Wetness Project Phase 3 Atmospheric Boundary Conditions (Experiment 1)*.

Kleinman, Benny, Liu, Ernest, and Redding, Stephen J. (2023). "Dynamic Spatial General Equilibrium". *Econometrica* 91.2, pp. 385 –424.

Krusell, Per and Smith Anthony A, Jr. (2022). *Climate Change Around the World*. Working Paper 30338. National Bureau of Economic Research.

Lange, et al. (May 5, 2021a). *WFDE5 over Land Merged with ERA5 over the Ocean (W5E5 v2.0)*. Version 2.0.

Lange, Stefan (July 17, 2019). "Trend-Preserving Bias Adjustment and Statistical Downscaling with ISIMIP3BASD (v1.0)". *Geoscientific Model Development* 12.7, pp. 3055–3070.

— (Apr. 14, 2021b). *ISIMIP3BASD*. Version 2.5.0. Zenodo.

Mengel, Matthias, Treu, Simon, Lange, Stefan, and Frieler, Katja (Aug. 20, 2021). "ATTRICI v1.1 – Counterfactual Climate for Impact Attribution". *Geoscientific Model Development* 14.8, pp. 5269–5284.

New, M, Lister, D, Hulme, M, and Makin, I (2002). "A High-Resolution Data Set of Surface Climate over Global Land Areas". *Climate Research* 21, pp. 1–25.

Phan, Toan and Schwartzman, Felipe (2023). "Climate Defaults and Financial Adaptation". *FRBR Working Paper.*

Rayner, N. A. (2003). "Global Analyses of Sea Surface Temperature, Sea Ice, and Night Marine Air Temperature since the Late Nineteenth Century". *Journal of Geophysical Research* 108.D14, p. 4407.

Reiter, Michael (2009). "Solving heterogeneous-agent models by projection and perturbation". *Journal of Economic Dynamics and Control* 33.3, pp. 649–665.

Roth Tran, Brigitte and Wilson, Daniel (2023). "The Local Economic Impact of Natural Disasters". *FRBSF Working Paper*.

Rudik, Ivan, Lyn, Gary, Tan, Weiliang, and Ortiz-Bobea, Ariel (2022). "The Economic Effects of Climate Change in Dynamic Spatial Equilibrium".

Schneider, et al. (Jan. 2014). "GPCC's New Land Surface Precipitation Climatology Based on Quality-Controlled in Situ Data and Its Role in Quantifying the Global Water Cycle". *Theoretical and Applied Climatology* 115.1-2, pp. 15–40.

— (2018). *GPCC Full Data Monthly Version 2018.0 at 0.5°: Monthly Land-Surface Precipitation from Rain-Gauges Built on GTS-based and Historic Data: Gridded Monthly Totals.* gzip compressed NetCDF. Version 2018.

Yoshimura, Kei and Kanamitsu, Masao (Aug. 1, 2008). "Dynamical Global Downscaling of Global Reanalysis". *Monthly Weather Review* 136.8, pp. 2983–2998.

A   Derivations: setup

A.1   Static equilibrium

We solve for equilibrium prices and quantities as functions of the local capital stock K_{it} and local number of workers N_{it}. Combining labor demand in final good and building production, we obtain $\varpi\alpha\frac{B_{it}}{N_{it}^B} = (1-\alpha)\frac{S_{it}}{N_{it}^P}$. Housing demand rewrites $\beta(1-\alpha)N_{it}\frac{S_{it}}{N_{it}^P} = \alpha H_{it}$.

We look for shares x, y such that

$$N_{it}^P = xN_{it} \quad , \quad H_{it} = yB_{it} \tag{20}$$

and so $N_{it}^B = (1-x)N_{it}$ and $S_{it} = (1-y)B_{it}$. Substituting into the previous equations, we obtain $\frac{\varpi\alpha}{1-\alpha} = \frac{(1-y)(1-x)}{x}$ and $\frac{\beta(1-\alpha)}{\alpha} = \frac{xy}{1-y}$. These two equations imply[43]

$$x = \frac{(1-\alpha)(1-\varpi\beta)}{\alpha\varpi + (1-\alpha)} \quad , \quad y = \beta\frac{(1-\alpha)+\alpha\varpi}{\alpha+(1-\alpha)\beta} \quad , \quad 1-y = \alpha\frac{1-\beta\varpi}{\alpha+(1-\alpha)\beta}. \tag{21}$$

Using these shares, we express the wage and the rental rate as

$$w_{it} = (1-\alpha)\alpha^\alpha\Xi^{-\alpha}Z_{it}(B_{it}/N_{it})^\alpha \quad , \quad r_{it} = \alpha^\alpha\Xi^{1-\alpha}Z_{it}(B_{it}/N_{it})^{-(1-\alpha)}, \tag{22}$$

where $\Xi = (1-\alpha)\frac{\alpha+(1-\alpha)\beta}{\alpha\varpi+(1-\alpha)}$. Before proceeding, it is useful to substitute out buildings and express prices in terms of capital:

$$w_{it} = w_{i0}Z_{it}L_i^{\omega\alpha}(K_{it}^{1-\omega-\varpi}N_{it}^{\varpi-1})^\alpha \quad , \quad r_{it} = r_{i0}Z_{it}L_i^{-\omega(1-\alpha)}(K_{it}^{1-\omega-\varpi}N_{it}^{\varpi-1})^{-(1-\alpha)},$$

where $w_{i0} = (1-\alpha)\alpha^\alpha\Xi^{-\alpha}(1-x)^{\varpi\alpha}$, $r_{i0} = \alpha^\alpha\Xi^{1-\alpha}(1-x)^{-(1-\alpha)\varpi}$.

We now solve for the rental rate of capital:

$$
\begin{aligned}
R_{K,it} &= (1-\omega-\varpi)(1-x)^\varpi K_{it}^{-(\omega+\varpi)}L_i^\omega N_{it}^\varpi r_{it} \\
&= (1-\omega-\varpi)\alpha^\alpha\Xi^{1-\alpha}(1-x)^{\alpha\varpi}Z_{it}L_i^{\omega\alpha}K_{it}^{-\phi}N_{it}^{1-\alpha+\alpha\varpi} \\
&= \underbrace{(1-\omega-\varpi)\alpha^\alpha\Xi^{1-\alpha}(1-x)^{\alpha\varpi}Z_iL_i^{\omega\alpha}}_{\equiv R_{0i}}e^{\chi_{it}}K_{it}^{-\phi}N_{it}^\psi \\
&= R_{0i}e^{\chi_{it}}K_{it}^{-\phi}N_{it}^\psi \\
&\equiv R_i(\chi_{it}, K_{it}, N_{it}),
\end{aligned}
$$

where $\phi = \omega + \varpi + (1-\omega-\varpi)(1-\alpha)$ and $\psi = 1 - \alpha + \alpha\varpi$. Turning to worker consumption (the real

---

[43]Multiplying both equations leads to $y(1-x) = \varpi\beta$ which can then be substituted into either of of the equations.

51

wage) in location i, we obtain:

$$
\begin{aligned}
C_{it} &= \frac{w_{it}}{r_{it}^{\beta}} \\[2mm]
&= \frac{(1-\alpha)\alpha^{\alpha}\Xi^{-\alpha}(1-x)^{\varpi\alpha}Z_{it}L_i^{\omega\alpha}(K_{it}^{1-\omega-\varpi}N_{it}^{\varpi-1})^{\alpha}}{\left[\alpha^{\alpha}\Xi^{1-\alpha}(1-x)^{-(1-\alpha)\varpi}Z_{it}L_i^{-\omega(1-\alpha)}(K_{it}^{1-\omega-\varpi}N_{it}^{\varpi-1})^{-(1-\alpha)}\right]^{\beta}} \\[2mm]
&= (1-\alpha)\alpha^{\alpha(1-\beta)}\Xi^{-\xi}(1-x)^{\varpi\xi}Z_{it}^{1-\beta}L_i^{\omega\xi}K_{it}^{(1-\omega-\varpi)\xi}N_{it}^{-\xi(1-\varpi)} \\[2mm]
&= \underbrace{(1-\alpha)\alpha^{\alpha(1-\beta)}\Xi^{-\xi}(1-x)^{\varpi\xi}Z_i^{1-\beta}L_i^{\omega\xi}}_{\equiv C_{0i}} \cdot e^{(1-\beta)\chi_{it}}\left(\frac{K_{it}^{1-\omega-\varpi}}{N_{it}^{1-\varpi}}\right)^{\xi} \\[2mm]
&\equiv C_{0i}e^{(1-\beta)\chi_{it}}\left(\frac{K_{it}^{1-\omega-\varpi}}{N_{it}^{1-\varpi}}\right)^{\xi}
\end{aligned}
$$

where $\xi = \alpha + \beta(1-\alpha)$. With consumption at hand, we express the flow utility in location i at time t:

$$
A_{it} + u\left(\frac{w_{it}}{r_{it}^{\beta}}\right) = A_i + a_{it} + u\left(C_{0i}e^{(1-\beta)\chi_{it}}\left(\frac{K_{it}^{1-\omega-\varpi}}{N_{it}^{1-\varpi}}\right)^{\xi}\right) \equiv U_i(a_{it}, \chi_{it}, K_{it}, N_{it}).
$$

A.2 Capitalists

We denote by $Y_{it}(I, K) = R_{K,it}K - c_i(I/K)K$ the net income of a capitalist with capital stock K investing I. We first guess and verify that $\mathcal{P}_{it}(K, b) = \Pi_{it}(K) + b + \mathcal{T}_{it}$, where $\Pi_{it}(K)$ reflects the permanent income of capitalists from capital returns, and $\mathcal{T}_{it}$ reflects the present discounted value of transfers from the national mutual fund. Substituting our guess into the capitalist problem (6), we obtain

$$
\rho\Pi_{it}(K) = \max_{I} Y_{it}(I, K) + (I - \delta_{it}K)\frac{\partial\Pi_{it}}{\partial K}(K) + \frac{\mathbb{E}_t[d_t\Pi_{it}]}{dt} \quad, \quad \rho = \overline{R}_t \quad, \quad \rho\mathcal{T}_{it} = \theta_{it} + \frac{\mathbb{E}_t[d_t\mathcal{T}_{it}]}{dt}. \quad (23)
$$

Thus, investment decisions are independent from bond holdings b and from transfers. We further guess and verify that $\Pi_{it}(K) = Q_{it}K$. Substituting this guess in (23), the investment policy becomes $c_i'(I/K) = Q_{it}$ and so $I = (c_i')^{-1}(Q_{it})K$.

Using our guess, the investment policy and the functional form of the investment cost in (23), we obtain

$$
(\rho + \delta_{it})Q_{it} = R_{K,it} + \frac{c_{i0}Q_{it}^{1+\zeta}}{1+\zeta} + \frac{\mathbb{E}_t[d_tQ_{it}]}{dt}, \quad I^*(K, Q_{it}) = c_{i0}Q_{it}^{\zeta}K.
$$

B Derivations: FAME

B.1 Flow payoffs

B.1.1 Workers

The flow payoffs become, to first order,

$$\frac{U_{it} - U_i^{SS}}{\epsilon} = a_{i1}(z + T_t^D) + u'(C_i^{SS})C_i^{SS} \cdot \left((1-\beta)\chi_{i1}(z + T_t^D) + \xi(1-\omega)\frac{k_i}{K_i^{SS}} - \frac{n_i}{N_i^{SS}} \right),$$

with $u'(C) = C^{-\gamma}$. In vector notation,

$$\epsilon^{-1}(U_t - U^{SS}) = \mathbf{vec}\Big(a_{i1}\Big)(z + T_t^D) + \mathbf{diag}\Big(u'(C_i^{SS})C_i^{SS}\Big)\Big[(1-\beta)\mathbf{vec}(\chi_{i1})(z + T_t^D)$$

$$+ \xi(1-\omega)\mathbf{diag}\Big(1/K_i^{SS}\Big)k - \xi\mathbf{diag}\Big(1/N_i^{SS}\Big)n\Big]$$

$$\equiv D_{UZ}z + D_{UT}T_t + D_{UK}k - D_{UN}n,$$

where we have defined

$$D_{UT} = D_{UZ} = \mathbf{vec}\Big(a_{i1} + u'(C_i^{SS})C_i^{SS}(1-\beta)\chi_{i1}\Big)$$

$$D_{UK} = \xi(1-\omega-\varpi)\mathbf{diag}\Big(u'(C_i^{SS})C_i^{SS}/K_i^{SS}\Big)$$

$$D_{UN} = \xi(1-\varpi)\mathbf{diag}\Big(u'(C_i^{SS})C_i^{SS}/N_i^{SS}\Big).$$

B.1.2 Capitalists

Similarly, to first order and in vector notation,

$$\epsilon^{-1}\left[\left(R_{K,it} + \frac{c_{i0}Q_{it}^{1+\zeta}}{1+\zeta} - \Delta_{it}Q_{it} \right) - \left(R_{K,i}^{SS} + \frac{c_{i0}(Q_i^{SS})^{1+\zeta}}{1+\zeta} - \Delta_i Q_i^{SS} \right) \right]_{i=1}^{\mathcal{I}}$$

$$= D_{RK}k - D_{RN}n + D_{CQ}\big[q^N n + q^K k + q^Z + q^T\big] - D_{QT}T_t^D - D_{QZ}z,$$

where

$$D_{RK} = -\phi\mathbf{diag}\Big(R_i^{SS}/K_i^{SS}\Big) \qquad\qquad D_{RN} = -\psi\mathbf{diag}\Big(R_i^{SS}/N_i^{SS}\Big)$$

$$D_{CQ} = \mathbf{diag}\Big(c_{i0}(Q_i^{SS})^{\zeta} - \Delta_i\Big) \qquad\qquad D_{QT} = D_{QZ} = \mathbf{vec}\Big(\delta_{i1}Q_i^{SS} - R_i^{SS}\chi_{i1}\Big)$$

B.2 Continuation value from migration

Denote by M the steady-state matrix $M(V^{SS})$. The continuation value from migration becomes, to leading order,

$$\frac{\mathcal{M}[V] - \mathcal{M}[V^{SS}]}{\epsilon} = Mv^N n + Mv^K k + Mv^Z z + Mv_t^T.$$

B.3 Continuation value from changes in population distribution

To linearize the law of motion of population, first note that

$$\frac{\partial m_{ji}}{\partial V_k} = \begin{cases} -\nu m_{ji} m_{jk} & \text{if } i \neq k \\ \nu m_{ji}(1 - m_{ji}) & \text{if } i = k \end{cases}$$

and so

$$M_{ij}^*(V + dV) = M_{ij}^*(V) + \mu \sum_k \frac{\partial m_{ji}}{\partial V_k} dV_k = M_{ij}^*(V) + \mu \nu m_{ji} \Big\{ dV_i - [m \cdot dV]_j \Big\}.$$

Then to leading order,

$$
\begin{aligned}
M_i^*(V + dV)[N^{SS}] &= M_i^*(V)[N^{SS}] + \mu \nu \sum_j m_{ji} \Big\{ dV_i - [m \cdot dV]_j \Big\} N_j^{SS} \\
&= M_i^*(V)[N^{SS}] + \nu \mu \Big[\Big(\mathbf{diag}(m^* N^{SS}) - m^* \mathbf{diag}(N^{SS}) m \Big) \cdot dV \Big]_i \\
&\equiv M_i^*(V)[N^{SS}] + (G \cdot dV)_i
\end{aligned}
$$

where $G = \nu \mu \Big(\mathbf{diag}(m^* N^{SS}) - m^* \mathbf{diag}(N^{SS}) m \Big)$. In vector notation, to leading order,

$$\epsilon^{-1} \left(\sum_j \frac{\partial V_i}{\partial N_j} (M^*(V)N)_j \right)_{i=1}^{I} = v^N M^* n + v^N G \big(v^N n + v^K k + v^Z z + v_t^T \big)$$

Similarly,

$$\epsilon^{-1} \left(\sum_j \frac{\partial Q_i}{\partial N_j} (M^*(V)N)_j \right)_{i=1}^{I} = q^N M^* n + q^N G \big(v^N n + v^K k + v^Z z + v_t^T \big)$$

54

B.4   Continuation value from changes in capital distribution

We obtain, to leading order,

$$
\begin{aligned}
\epsilon^{-1} \sum_j \frac{\partial V_i}{\partial K_j} K_j \left(c_{j0} Q_j^\zeta - \Delta_{jt} \right) &= \sum_j v_{ij}^K K_j^{SS} \left\{ \epsilon^{-1} dI_j^* - \delta_{1j}(z + T_t^D) \right\} \\
&= \sum_j v_{ij}^K K_j^{SS} \left\{ \zeta c_{j0} (Q_j^{SS})^{\zeta-1} \left[\sum_j q_{j\ell}^N n_\ell + \sum_\ell q_{j\ell}^K k_\ell + q_j^Z z + q_{tj}^T \right] - \delta_{j1}(z + T_t^D) \right\} \\
&= v^K \left\{ \mathrm{D}_{IQ} \left[q^N n + q^K k + q^Z z + q_t^T \right] - (z + T_t^D) \mathrm{D}_{\Delta T} \right\}
\end{aligned}
$$

where

$$
\mathrm{D}_{IQ} = \zeta \, \mathbf{diag}\left(K_j^{SS} c_{j0} (Q_j^{SS})^{\zeta-1} \right) \qquad\qquad \mathrm{D}_{\Delta T} = \mathbf{vec}\left(K_j^{SS} \delta_{j1} \right)
$$

Similarly, to leading order,

$$
\left(\epsilon^{-1} \sum_j \frac{\partial Q_i}{\partial K_j} K_j \left(c_{j0} Q_j^\zeta - \Delta_{jt} \right) \right)_i = q^K \left\{ \mathrm{D}_{IQ} \left[q^N n + q^K k + q^Z z + q_t^T \right] - (z + T_t^D) \mathrm{D}_{\Delta T} \right\}
$$

B.5   FAME in vector notation

B.5.1   Workers

Thus, the linearized master equation for the worker value becomes, in vector notation,

$$
\rho \left(v^N n + v^K k + v^Z z + v^T \right) - \frac{\partial v^T}{\partial t}
$$

$$
= \underbrace{\mathrm{D}_{UZ} z + \mathrm{D}_{UT} T_t^D + \mathrm{D}_{UK} k - \mathrm{D}_{UN} n}_{\text{flow payoff}} + \underbrace{M \left(v^N n + v^K k + v^Z z + v^T \right)}_{\text{continuation value from migration}} + \underbrace{\mathcal{A}(z)[v^Z z]}_{\text{c.v. from climate shocks}}
$$

$$
+ \underbrace{v^N M^* n + v^N G \left(v^N n + v^K k + v^Z z + v^T \right)}_{\text{continuation value from changes in the population distribution}} + \underbrace{v^K \left\{ \mathrm{D}_{IQ} \left[q^N n + q^K k + q^Z z + q^T \right] - (z + T_t^D) \mathrm{D}_{\Delta T} \right\}}_{\text{continuation value from changes in the capital distribution}}
$$

We impose that z_t follows an AR(1) process: $\mathcal{A}(z)[V] = -\theta z V'(z) + \frac{z^2}{2} V''(z)$. Identifying coefficients, and with unknowns in bold notation,

$$
\begin{aligned}
\rho \boldsymbol{v^N} &= -\mathrm{D}_{UN} + M\boldsymbol{v^N} + \boldsymbol{v^N} M^* + \boldsymbol{v^N} G \boldsymbol{v^N} + \boldsymbol{v^K} \mathrm{D}_{IQ} \boldsymbol{q^N} \\
\rho \boldsymbol{v^K} &= \mathrm{D}_{UK} + M\boldsymbol{v^K} + \boldsymbol{v^N} G \boldsymbol{v^K} + \boldsymbol{v^K} \mathrm{D}_{IQ} \boldsymbol{q^K} \\
\rho \boldsymbol{v^Z} &= \mathrm{D}_{UZ} + M\boldsymbol{v^Z} - \theta \boldsymbol{v^Z} + \boldsymbol{v^N} G \boldsymbol{v^Z} + \boldsymbol{v^K} \mathrm{D}_{IQ} \boldsymbol{q^Z} - \boldsymbol{v^K} \mathrm{D}_{\Delta T} \\
\rho \boldsymbol{v^T} - \frac{\partial \boldsymbol{v^T}}{\partial t} &= \mathrm{D}_{UT} T_t^D + M\boldsymbol{v^T} + \boldsymbol{v^N} G \boldsymbol{v^T} + \boldsymbol{v^K} \mathrm{D}_{IQ} \boldsymbol{q^T} - \boldsymbol{v^K} \mathrm{D}_{\Delta T} T_t^D .
\end{aligned}
$$

B.5.2 Capitalists

Similarly, the linearized master equation for capitalists becomes, in vector notation,

$$\rho\big(q^N n + q^K k + q^Z z + q^T\big) - \frac{\partial q^T}{\partial t}$$

$$\underbrace{}_{\text{flow payoff}}$$

$$= \underbrace{\mathrm{D}_{RK}k - \mathrm{D}_{RN}n + \mathrm{D}_{CQ}\big[q^N n + q^K k + q^Z z + q^T\big] - \mathrm{D}_{QT}T_t^D - \mathrm{D}_{QZ}z +}_{} \quad \overbrace{\mathcal{A}(z)[q^Z z]}^{\text{c.v. from climate shocks}}$$

$$+ \quad \underbrace{q^N M^* n + q^N G\big(v^N n + v^K k + v^Z z + v^T\big)}_{\text{continuation value from changes in the population distribution}}$$

$$+ \quad \underbrace{q^K\Big\{\mathrm{D}_{IQ}\big[q^N n + q^K k + q^Z z + q^T\big] - (z + T_t^D)\mathrm{D}_{\Delta T}\Big\}}_{\text{continuation value from changes in the capital distribution}}$$

Identifying coefficients, and with unknowns in bold notation,

$$\rho \boldsymbol{q^N} = -\mathrm{D}_{RN} + \mathrm{D}_{CQ}\boldsymbol{q^N} + \boldsymbol{q^N}M^* + \boldsymbol{q^N}G\boldsymbol{v^N} + \boldsymbol{q^K}\mathrm{D}_{IQ}\boldsymbol{q^N}$$

$$\rho \boldsymbol{q^K} = \mathrm{D}_{RK} + \mathrm{D}_{CQ}\boldsymbol{q^K} + \boldsymbol{q^N}G\boldsymbol{v^K} + \boldsymbol{q^K}\mathrm{D}_{IQ}\boldsymbol{q^K}$$

$$\rho \boldsymbol{q^Z} = -\mathrm{D}_{QZ} + \mathrm{D}_{CQ}\boldsymbol{q^Z} - \theta\boldsymbol{q^Z} + \boldsymbol{q^N}G\boldsymbol{v^Z} + \boldsymbol{q^K}\mathrm{D}_{IQ}\boldsymbol{q^Z} - \boldsymbol{q^K}\mathrm{D}_{\Delta T}$$

$$\rho \boldsymbol{q^T} - \frac{\partial \boldsymbol{q^T}}{\partial t} = -\mathrm{D}_{QT}T_t^D + \mathrm{D}_{CQ}\boldsymbol{q^T} + \boldsymbol{q^N}G\boldsymbol{v^T} + \boldsymbol{q^K}\mathrm{D}_{IQ}\boldsymbol{q^T} - \boldsymbol{q^K}\mathrm{D}_{\Delta T}T^D(t)$$

Collecting terms for $\boldsymbol{v^N}, \boldsymbol{v^K}, \boldsymbol{q^N}, \boldsymbol{q^K}$, Proposition 2 obtains. Collecting terms for $\boldsymbol{v^T}, \boldsymbol{q^T}$, Proposition 3 obtains. The stochastic FAME writes

$$(\rho + \theta)\begin{pmatrix} \boldsymbol{v^Z} \\ \boldsymbol{q^Z} \end{pmatrix} = \begin{pmatrix} \mathrm{D}_{UZ} - v^K \mathrm{D}_{\Delta T} \\ -\mathrm{D}_{QZ} - q^K \mathrm{D}_{\Delta T} \end{pmatrix} + \begin{pmatrix} M + v^N G & v^K \mathrm{D}_{IQ} \\ q^N G & \mathrm{D}_{CQ} + q^K \mathrm{D}_{IQ} \end{pmatrix}\begin{pmatrix} \boldsymbol{v^Z} \\ \boldsymbol{q^Z} \end{pmatrix}. \tag{24}$$

This is now a standard matrix equation.

B.6 Welfare

B.6.1 Proof of Proposition 5

Omit time subscripts and steady-state superscripts for simplicity. Totally differentiating aggregate welfare, we obtain:

$$d\overline{V} = \sum_i \Big[N_i dV_i + V_i dN_i\Big] = \underbrace{\mathbb{E}_N[dV_i]}_{\text{expectation}} + \underbrace{\mathbb{Cov}_N\left[\frac{dN_i}{N_i}, V_i\right]}_{\text{covariance}}$$

We can further characterize the expectation component:

$$
\begin{aligned}
\epsilon^{-1}\mathbb{E}_N[dV_i] &= \sum_i N_i \left(v_i^T + \sum_j v_{ij}^N dN_j + \sum_j v_{ij}^K dK_j \right) \\
&= \sum_i N_i v_i^T + \sum_j \left(\sum_i N_i v_{ij}^N \right) dN_j + \sum_j \left(\sum_i N_i v_{ij}^K \right) dK_j \\
&= \mathbb{E}_N[v_i^T] + \mathbb{E}_N \left[\varepsilon_j^{vN} \frac{dN_j}{N_j} \right] + \mathbb{E}_K \left[\varepsilon_j^{vK} \frac{dK_j}{K_j} \right],
\end{aligned}
$$

where we defined $\varepsilon_j^{vN} \equiv \sum_i N_i v_{ij}^N$ and $\varepsilon_j^{vK} \equiv \sum_i N_i v_{ij}^K$. Then,

$$
\mathbb{E}_N \left[\varepsilon_j^{vN} \frac{dN_j}{N_j} \right] = \mathbb{C}\text{ov}_N \left[\varepsilon_j^{vN}, \frac{dN_j}{N_j} \right] + \mathbb{E}_N \left[\varepsilon_j^{vN} \right] \mathbb{E}_N \left[\frac{dN_j}{N_j} \right] = \mathbb{C}\text{ov}_N \left[\varepsilon_j^{vN}, \frac{dN_j}{N_j} \right].
$$

In addition,

$$
\mathbb{E}_K \left[\varepsilon_j^{vK} \frac{dK_j}{K_j} \right] = \mathbb{C}\text{ov}_K \left[\varepsilon_j^{vK}, \frac{dK_j}{K_j} \right] + \mathbb{E}_K \left[\varepsilon_j^{vK} \right] \mathbb{E}_K \left[\frac{dK_j}{K_j} \right] = \mathbb{C}\text{ov}_K \left[\varepsilon_j^{vK}, \frac{dK_j}{K_j} \right] + \mathbb{E}_K \left[\varepsilon_j^{vK} \right] d\bar{K},
$$

which concludes the proof of the first part of the proposition. For the proof of the second part, note that

$$
d\overline{\mathcal{W}}_t = \sum_i N_i^{SS} d\mathcal{W}_{it} + \sum_i dN_{it} \mathcal{W}_i^{SS} = \sum_i N_i^{SS} dV_{it} + \sum_i dN_{it} \mathcal{W}_i^{SS},
$$

where the second line uses the steady-state determination of population.

B.6.2   Consumption equivalent welfare

For any period τ, we compute consumption equivalent welfare change between the steady-state SS and any counterfactual as $\omega_{i\tau}$, such that

$$
\mathbb{E}_\tau \int_\tau^\infty e^{-\rho(t-\tau)} \left\{ A_{i(t)}^{SS} + \varepsilon_{i(t)t} + u((1+\omega_{i\tau})C_{i(t)}^{SS}) \right\} dt = \mathbb{E}_\tau \int_\tau^\infty e^{-\rho(t-\tau)} \left\{ A_{i(t),t} + u(C_{i(t),t}) \right\} dt
$$

where ε_{it} denotes the preference shock for the current (chosen) location.

Worker welfare: lump-sum preference shocks   We start with the definition of welfare when preference shocks are 'lump-sum', that is, when they are realized upon moving. In that case, preference shocks are not included in the welfare metric, which simply becomes V_{it} in location i at time t.

   Log utility.   Under log utility $\gamma = 1$, we obtain

$$
V_i^{SS} + \rho^{-1} \log(1 + d\omega_{i\tau}) = V_{i\tau} \iff d\omega_{i\tau} = e^{\rho(V_{i\tau} - V_i^{SS})} - 1.
$$

When shocks are small $\epsilon \to 0$, to a first order,

$$d\omega_{i\tau} = \rho \ dV_{i\tau} \tag{25}$$

CRRA utility. With CRRA utility when $\gamma \neq 1$, $u(C) = \frac{C^{1-\gamma}-1}{1-\gamma}$,

$$V_i^{A,SS} + (1 + d\omega_{i\tau})^{1-\gamma} V_{i\tau}^{C,SS} - \frac{1}{\rho(1-\gamma)} = V_{i\tau},$$

where

$$V_i^{A,SS} = \mathbb{E}_0 \int_0^\infty e^{-\rho t} \left\{ A_{i(t)}^{SS} \right\} dt \implies (\rho + \mu) V_i^{A,SS} = A_i^{SS} + \mu \sum_j m_{ij} V_j^{A,SS}$$

$$V_i^{C,SS} = \mathbb{E}_0 \int_0^\infty e^{-\rho t} \frac{(C_{i(t)}^{SS})^{1-\gamma}}{1-\gamma} dt \implies (\rho + \mu) V_i^{C,SS} = \frac{(C_i^{SS})^{1-\gamma}}{1-\gamma} + \mu \sum_j m_{ij} V_j^{C,SS}.$$

Then

$$(1 + d\omega_{i\tau})^{1-\gamma} V_{i\tau}^{C,SS} - V_i^{C,SS} = V_{i\tau} - V_i^{SS} \iff d\omega_{i\tau} = \left(1 + \frac{V_{i\tau} - V_i^{SS}}{V_i^{C,SS}} \right)^{\frac{1}{1-\gamma}} - 1$$

When shocks are small $\epsilon \to 0$, to a first order,

$$d\omega_{i\tau} = \frac{1}{1-\gamma} \frac{dV_{i\tau}^{IRF}}{V_i^{C,SS}} = \frac{\rho \ dV_{i\tau}^{IRF}}{\widetilde{V}_i}, \tag{26}$$

where

$$\widetilde{V}_i = \rho \mathbb{E}_0 \int_0^\infty e^{-\rho t} (C_{i(t)}^{SS})^{1-\gamma} dt \implies (\rho + \mu) \widetilde{V}_i = \rho (C_i^{SS})^{1-\gamma} + \mu \sum_j m_{ij} \widetilde{V}_j.$$

Aggregate welfare Aggregate welfare is defined as

$$\overline{V}_t = \sum_i N_{it} V_{it} \ , \ \overline{Q}_t = \sum_i K_{it} Q_{it}.$$

Derivations and formulas are identical to the local welfare case above after replacing local values with aggregate values.

Worker welfare: permanent preference shocks

Log utility. When preference shocks are permanent until the next moving opportunity, then local welfare is given by

$$\mathcal{W}_i[V_t] = \frac{1}{\nu} \log \left(\sum_j e^{\nu(V_{jt} - \tau_{ij})} \right).$$

In response to a change, we have

$$d\mathcal{W}_i = \sum_j m_{ij} dV_{jt} = \left(m \cdot dV_t \right)_i.$$

Under log utility, similar derivations as above for small ϵ lead to

$$\left(m \cdot dV_t \right)_i = \left(m \cdot \left(\frac{d\omega_{i\tau}}{\rho} \right)_j \right)_i = \frac{d\omega_{i\tau}}{\rho},$$

so that

$$d\omega_{i\tau} = \rho \left(m \cdot dV_t \right)_i.$$

CRRA utility. Similar derivations as above lead to

$$d\omega_{i\tau} = \frac{\rho \left(m \cdot dV_t \right)_i}{\left(m \cdot \tilde{V} \right)_i}.$$

Aggregate worker welfare. Aggregate welfare is defined as $\overline{\mathcal{W}}_t = \sum_i N_{it} \mathcal{W}_{it}$.

Capitalist welfare. For capitalists we must take a stand on how claims to the national mutual fund are distributed—and hence land rents rebated. For simplicity, we assume that T_{it} is proportional to $\left(R_{K,it} + \frac{c_{i0} Q_{it}^\zeta}{1+\zeta} - \Delta_{it} Q_{it} \right) K_{it}$. Let $\bar{\pi}$ be this proportionality constant. Under this assumption, $\mathcal{T}_{it} = \bar{\pi} Q_{it} K_{it}$.

Because of linear utility, without loss we may pin down $b_{it} = 0$. Hence, capitalist welfare in location i at time t is $\mathcal{P}_{it} = (1 + \bar{\pi}) Q_{it} K_{it}$, and aggregate welfare is $\overline{\mathcal{P}}_t = \sum_i \mathcal{P}_{it}$.

C Steady-state computation

We solve for steady-state using the following algorithm:

1. Start by using (12) to solve for Q_i^{SS}

2. Given Q_i^{SS}, then use (10) to solve for the equilibrium capital as a function of population:

$$K_i^{SS} = R_{0i}^{1/\phi} \left(\rho Q_i^{SS} + \frac{\zeta c_{i0}(Q_i^{SS})^{1+\zeta}}{1+\zeta} \right)^{-1/\phi} (N_i^{SS})^{\psi/\phi} \equiv \mathcal{K}_i(N_i^{SS}) \tag{27}$$

3. Substitute (27) into (9) to obtain

$$\rho V_i^{SS} = U_i(\mathcal{K}_i(N_i^{SS}), N_i^{SS}) + \mathcal{M}_i[V^{SS}] \tag{28}$$

4. Iterate alternatively on (28) and (11) to jointly solve equilibrium values V_i^{SS} and population N_i^{SS}:

   (a) Start from a uniform guess for N_i^{SS} (or any other guess)

   (b) Solve (28) for V_i^{SS}

   (c) Update N_i^{SS} by solving (11) given V_i^{SS}

   (d) Keep iterating on (b-c) until both N_i^{SS} and V_i^{SS} have converged.

D   Reduced-form evidence

D.1   Trends in cold waves

Figure 13: 1-in-20-years cold waves and global mean temperature.
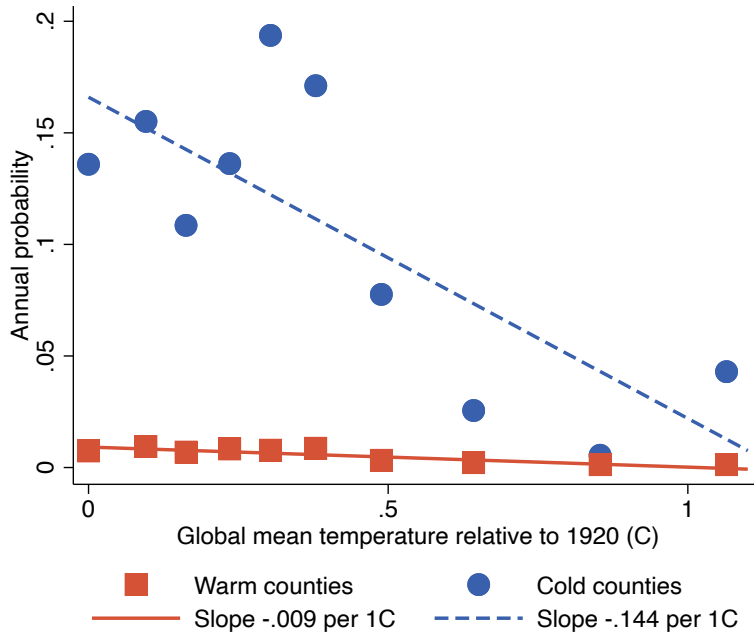
D.2 The impact of storms

Figure 14: The impact of 1-in-50-years-storms on economic activity in inland counties.

(a) Wage

(b) Income per capita

(c) Population

(d) Employment

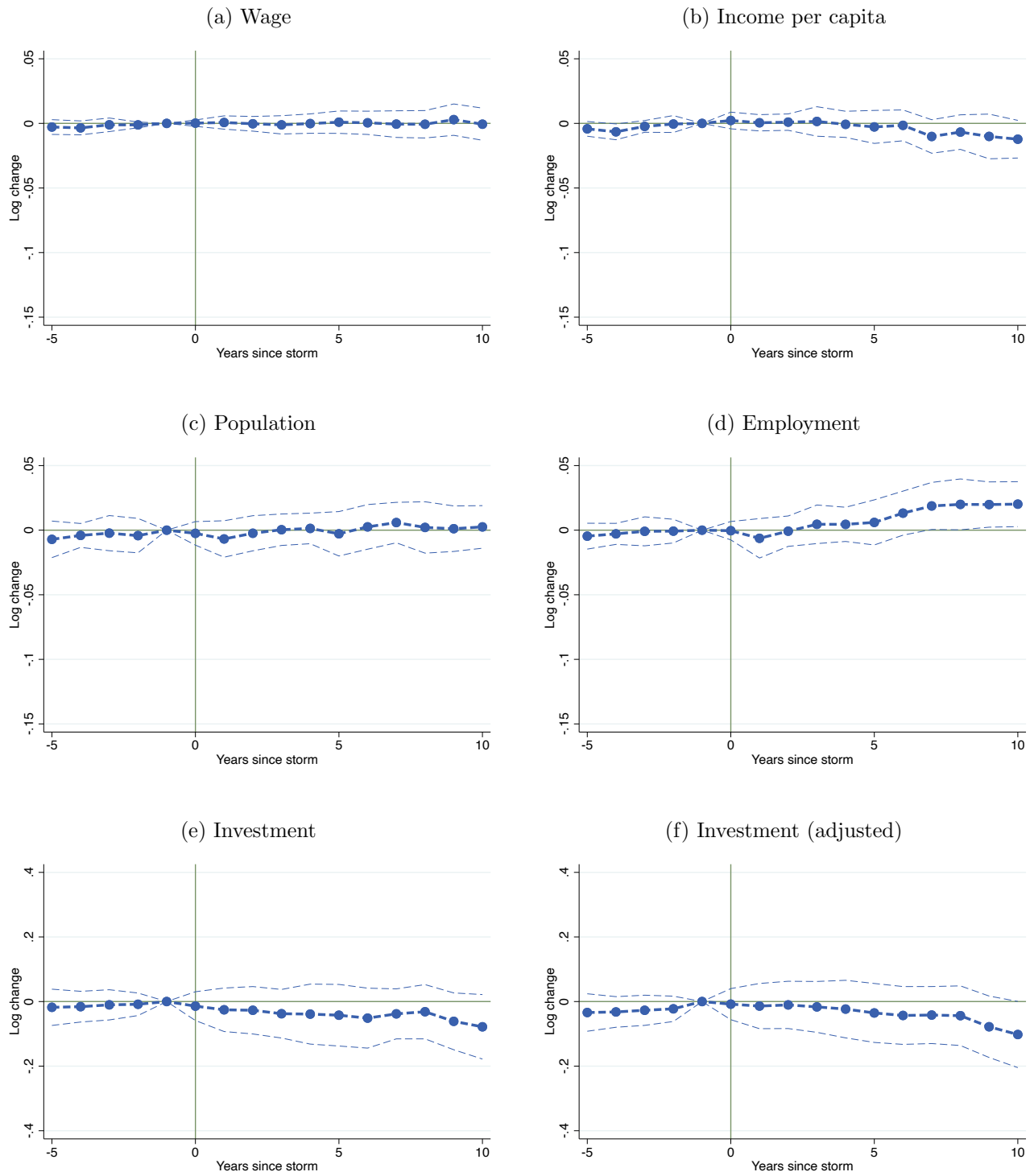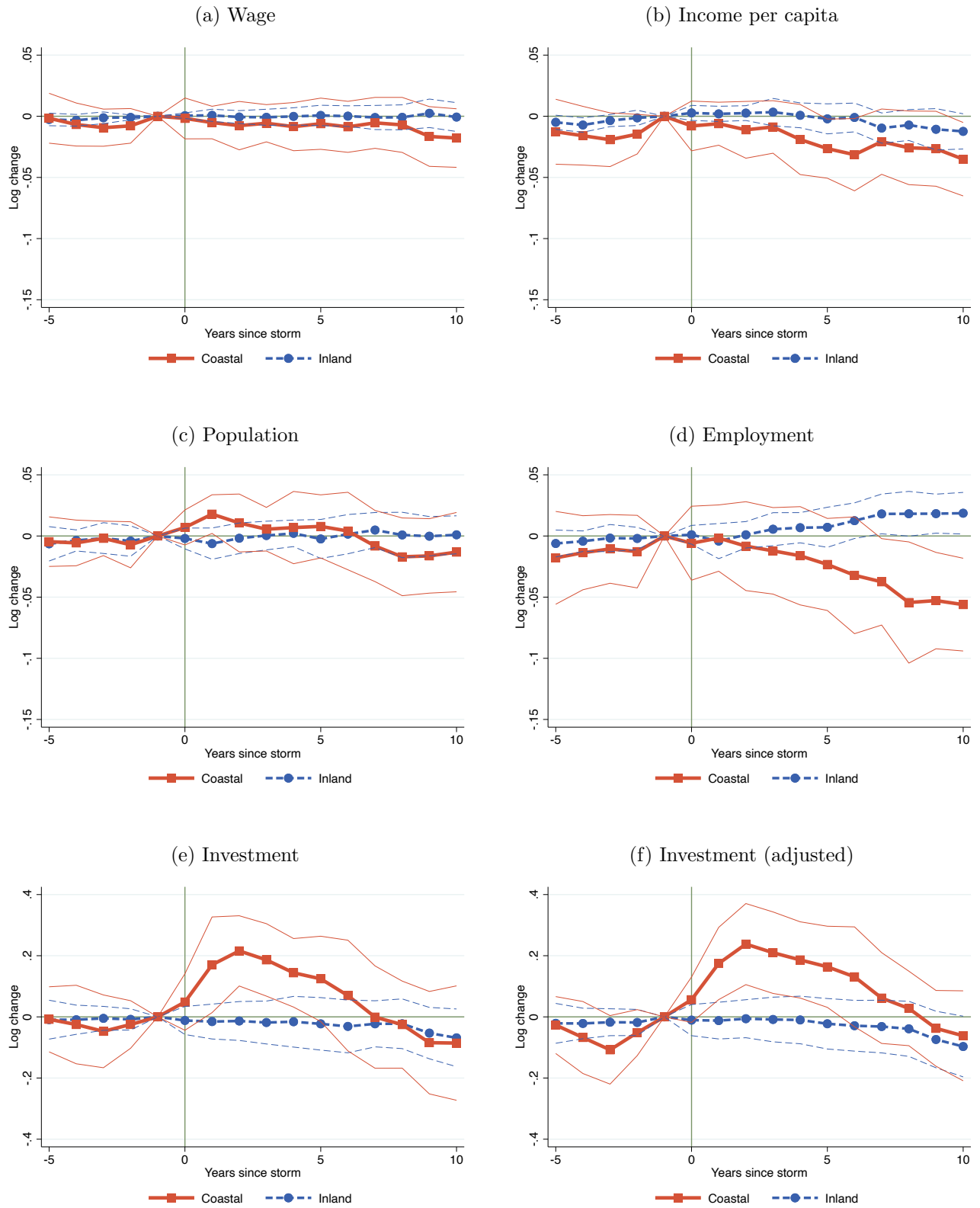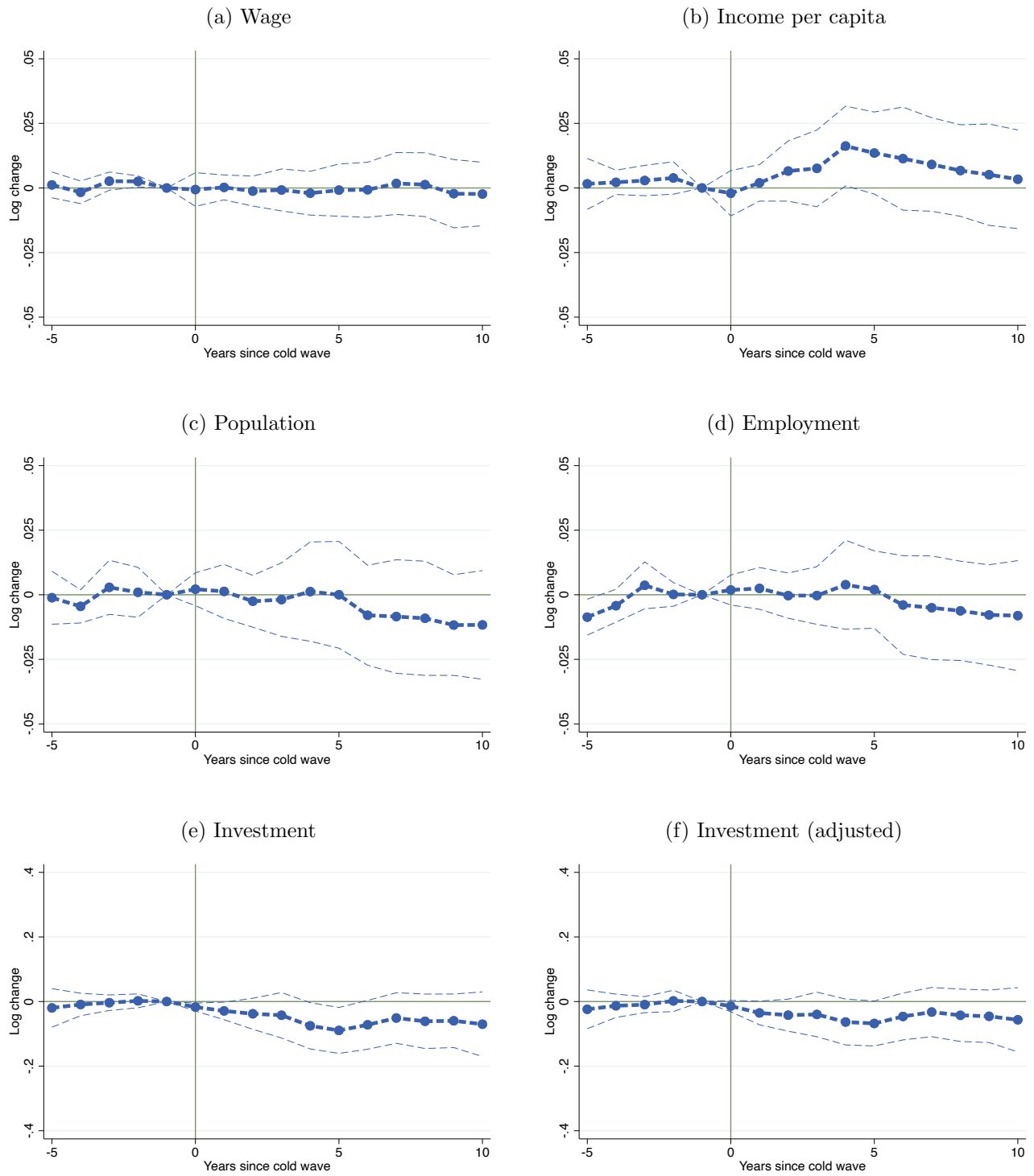(e) Investment

(f) Investment (adjusted)

Figure 15: The impact of 1-in-50-years-storms on economic activity in all counties.

D.3 The impact of cold waves

Figure 16: The impact of 1-in-20-years cold waves on economic activity in cold counties.

(a) Wage

(b) Income per capita

(c) Population

(d) Employment

(e) Investment

(f) Investment (adjusted)

E Estimation: Proof of Proposition 6

We use the steady-state investment rate (12) to obtain an estimate of the steady-state capital stock in each location: $K_i = \tilde{I}_i/\delta$. Next, we recover an estimate of the stock of buildings B_i and housing H_i from the constant shares rule (20)-(21) and the buildings production function:

$$B_i = L_i^\omega \left((1-x)N_i\right)^\varpi K_i^{1-\omega-\varpi} \quad , \quad H_i = yB_i$$

The wage equation (22) then delivers an estimate of fundamental productivity in county i:

$$Z_i = \frac{w_i}{(1-\alpha)\alpha^\alpha \Xi^{-\alpha}\left(B_i/N_i\right)^\alpha}.$$

From there we construct $R_{0i} = (1-\omega-\varpi)\alpha^\alpha \Xi^{1-\alpha}(1-x)^{\alpha\varpi}Z_i L_i^{\omega\alpha}$. Combining equations (10) and (12) then delivers local investment costs:

$$c_{i0} = \delta \left[\frac{1}{R_{0i}K_i^{-\phi}N_i^\psi}\left(\rho + \frac{\zeta\delta}{1+\zeta}\right)\right]^\zeta$$

Next, we construct $C_{0i} = (1-\alpha)\alpha^{\alpha(1-\beta)}\Xi^{-\xi}Z_i^{1-\beta}L_i^{\omega\xi}$ and so $u_{i0} = u\left(C_{0i}K_i^{(1-\omega-\varpi)\xi}N_i^{-(1-\varpi)\xi}\right)$ which implies $U_i = A_i + u_{i0}$.

To recover migration costs, we construct migration shares as $m_{ij} = \frac{\mathtt{m}_{ij}}{\sum_k \mathtt{m}_{ik}}$. The equation for migration shares (4) implies that $X_{ij} \equiv \log m_{ij} - \log m_{ii} = \nu(V_j - V_i) - \nu\tau_{ij} \equiv Y_j - Y_i + \varepsilon_{ij}$ after imposing the normalization $\tau_{ii} = 0$. We exploit that $X_{ij} + X_{ji} = \varepsilon_{ij} + \varepsilon_{ji}$. We assume symmetric migration costs $\tau_{ij} = \tau_{ji}$, which we then recover as

$$\tau_{ij} = -\frac{X_{ij} + X_{ji}}{2\nu}.$$

We are left with estimating local amenities. We proceed in two steps. The first step consists in recovering local valuations from the steady-state population distribution. Defining $X_i = e^{\nu V_i}$ and $\theta_{ki} = e^{-\nu\tau_{ki}}$, equation (11) implies, together with a normalization of values:

$$X_i = \frac{N_i}{\sum_k \frac{N_k \theta_{ki}}{\sum_j \theta_{kj}X_j}} \quad , \quad \sum_i X_i = 1. \tag{29}$$

The system of equations (29) satisfies the gross substitutes property, and so has at most one solution. A simple iterative method delivers the solution to equation (29), and we recover $V_i = \frac{1}{\nu}\log\left(X_i\right)$.

With an estimate of local valuations V_i at hand, the second step consists in inverting the HJB (3) to

Table 2: Impact of climate change on welfare and allocations without anticipations.

	Welfare				Allocations	
	Workers		Capitalists		Population	Capital
	2023	2100	2023	2100	2100	2100
No climate anticipations: Workers						
Aggregate (%)	-4.9	-11.6	-0.8	-13.4		-30.8
St.dev. (p.p.)	2.4	4.6	5.2	44.1	38.0	43.5
No climate anticipations: Capitalists						
Aggregate (%)	-4.9	-11.6	-0.5	-13.1		-30.6
St.dev. (p.p.)	2.4	4.2	4.4	45.6	39.9	45.0
No climate anticipations: Both						
Aggregate (%)	-4.8	-11.5	-0.5	-13.1		-29.5
St.dev. (p.p.)	2.4	4.7	3.9	43.1	36.9	42.4

recover amenities. In particular,

$$A_i = (\rho + \mu)V_i - \left(u_{i0} + \mathcal{M}_i[V] \right).$$

F Additional results

See Table 2 and Figure 17.

G Data description

G.1 Economic data

We use county-year population data from the BEA. The BEA constructs annual population data starting from the decennial Census population figures. They estimate population at intercensal dates using the Das Gupta method. Estimates are replaced with official Census intercensal figures as they are released, which are generated via the Das Gupta and location and demographic-specific adjustments.

Income per capita is measured as personal income from the BEA. It includes income of individuals, nonprofit institutions serving individuals, private noninsured welfare funds, private trust funds, transfer receipts, employer contributions to health and pensions plans, interest received, imputed incomes. Personal income excludes personal contributions for government social insurance, pension and annuity benefits from private and government employee pension plans, and income from interpersonal transfers. To measure wages, we use salary income from the BEA.

We also obtain employment from the BEA. They weight full-time and part time jobs.

Figure 17: Early learning of climate change.
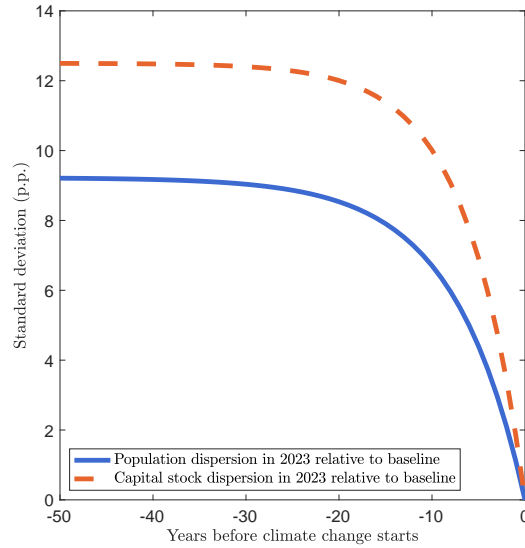
To measure investment, we use capital expenditures, which consists of total capital expenditures for the manufacturing sector from the Census of Manufacturers from 1958 to 1992, and the Economic Censuses from 1997 to 2012. The Census of Manufacturers reports are digitized via the ICPSR 2896 project. Economic Censuses are released with a lag. Presently, capital expenditures at the county level are available for 2002, 2007, and 2012. The economic census is conducted by the Census Bureau every 5 years and includes more than 4 million selected business locations to get metrics on the American economy. Because our measure of investment of available every 5 years only, we linearly interpolate between Census years prior to running our event studies.

We also collect information on local government expenditures from the Government Finance Database, which assembles and standardizes data provided by the Census of Governments. We use total government expenditures (Census codes E, F, G, L, and M) as a control in our analysis, that we linearly interpolate in between Census years.

G.2   ISIMIP3a data

The Inter-Sectoral Impact Model Intercomparison Project (ISIMIP) models the impacts of climate change on natural and human systems. ISIMIP simulation round 3a introduced several global, high-frequency datasets quantifying several atmospheric variables across the 20th and early 21st centuries. We use the observed climate dataset, spanning 1901-2019 at a $0.5° \times 0.5°$ resolution. This dataset harmonizes two constituent datasets, Global Soil Wetness Project Phase 3 (GSWP3, 1901-1978) (Kim, 2017) and WATCH Forcing Data methodology applied to ERA5 reanalysis dataset (W5E5, 1979-2019) (Lange, 2021a), each generated through a combination of numerical weather prediction (NWP) models and station-

level atmospheric observations (Mengel et al., 2021).

The foundation of the GSWP3 is the Twentieth Century Reanalysis Project dataset (20CR), covering 1871 to 2008 at a 2° resolution and 6-hour frequency. Using the NOAA's NCEP Global Forecast System to first simulate a suite of atmospheric variables, the resulting weather predictions are then disciplined using reported and derived surface and sea-level pressure observations via an Extended Kalman Filter data assimilation system (Cucchi, 2020). Lower boundary conditions used to run the NWP consist of sea surface temperature and sea-ice concentration from the UK Met Office HadISST1.1 dataset (Rayner, 2003) interpolated from monthly mean data to a daily frequency. Pressure observations for the data assimilation step were obtained from the International Surface Pressure Databank version 2 (Cram, 2015), which collates data from numerous international meteorological organizations.

Drawing from 20CR, GSWP3 was created by dynamically downscaling and applying bias-adjustment to several selected variables. Variables were first cast from a 2° to a roughly 0.5° resolution from 1901-2010 at a 3 hour frequency using a spectral nudging technique in a Global Spectral Model (Yoshimura and Kanamitsu, 2008). The downscaled dataset was then bilinearly interpolated to a regular 0.5° grid, with model biases further corrected by variable using observational data: Global Precipitation Climatology Centre Full Data Monthly Product Version 7 (Schneider, 2014) for precipitation; Climatic Research Unit CL2.0 (New et al., 2002) dataset for windspeed; and Climatic Research Unit TS3.23 (Harris, 2014) dataset for temperature, pressure, and humidity.

Similar to the bias-adjustments applied to 20CR in order to create GSWP3, W5E5 is built on the European Centre for Medium-Range Weather Forecast's (ECMWF) reanalysis dataset version 5 (ERA5) (Hersbach, 2020). ERA5 first leverages the ECMWF's Integrated Forecasting System Cycle 41r2 for numerical weather prediction. These modeled estimates are then reconciled with station-level observations to create a high-resolution dataset using a two-part data assimilation system: 1) the incremental 4D-Variable Assimilation method (Courtier et al., 1994) for atmospheric variables and ozone, and 2) a land data assimilation system comprising optimal interpolation schemes for temperature, relative humidity, and snow and a Simplified Extended Kalman Filter for soil moisture. The ensemble data assimilation incorporates approximately 96 billion observed data points across the complete dataset (1979-2019) from a plethora of sources, spanning conventional meteorological measurements to satellite data, around the globe. The final ERA5 dataset is at a resolution of 31km and an hourly frequency.

Following the framework for land surface models and global hydrological models set out by the EU WATCH program, time series from ERA5 were bias-corrected and aggregated to a 0.5° resolution to create the WATCH Forcing Data methodology applied to ERA5 reanalysis (WFDE5) (Cucchi, 2020) dataset. Adjustments to match observed monthly moments were applied using the Climatic Research Unit TS40.3 (Harris, 2020) dataset for surface air temperature, shortwave radiation, rainfall rate, and snowfall rate, and the Global Precipitation Climatology Centre Full Data Monthly Product Version 2018 (Schneider, 2018) for rainfall and snowfall rates. W5E5, used in the ISIMIP dataset, was created by

combining WFDE5 observations over land with ERA5 observations over the ocean (Lange, 2021a).

Inconsistent availability in the data used to produce 20CR, as well as in the subsequent bias-adjustment to generate GSWP3, produced known artifacts and spurious trends. Furthermore, many more observations were used for data assimilation in ERA5, and thus WFDE5, leading the authors of ISIMIP3a to consider W5E5 the more realistic dataset. In order to temporally extend W5E5 backward to 1901, GSWP3 data from 1901-1978 were homogenized with W5E5 to smooth discontinuities between the datasets at the 1978/1979 threshold. Within the common 1979-2004 reference period, GSWP3 time series were quantile mapped (Lange, 2019; Lange, 2021b) to match the distribution of the corresponding W5E5 time series. The resulting GSWP3-W5E5 dataset preserves the trends of the GSWP3 data and is identical to the original W5E5 data from 1979 onwards, but differs from the original 1901-1978 GSWP3 data.

G.3   Extreme event indicators

Heat—The 95th percentile of the annual mean temperature distribution in 1901-1910 is equal to 20°C. Importantly, an annual mean temperature of 20°C or above is highly correlated with extreme heat. For instance, the 95th percentile of daily maximum temperature is 33°C. The correlation between annual mean temperature and annual maximum temperature is high, at 0.71.

The 95th percentile of days spent above the 95th percentile of annual mean temperature for the 1901-1910 distribution is 20% of the year spent above 20°C. Crucially, this proportion is highly correlated with a high fraction of the year spent at much higher temperatures. The 95th percentile of days spent above the 95th percentile of maximum temperature for the 1901-1910 distribution is 18% of the year spent above 33°C. The correlation between these two fractions is substantial, at 0.91.

Storms—For comparison with our residualized percentiles, the 99th percentile of the un-residualized distribution of daily maximum windspeed for the years 1901-1910 is 10 meters per second (m/s). The largest windspeed is 18 m/s. Recall that these measures are daily averages, and thus allow for much faster gusts in small time windows. Similarly, the 99th percentile of the un-residualized distribution of daily maximum precipitation for the years 1901-1910 is 100 millimeters per day (mm/d). The maximum is above 220 mm/d.